Endocytóza

Endosomy, vakuola a ti druzí

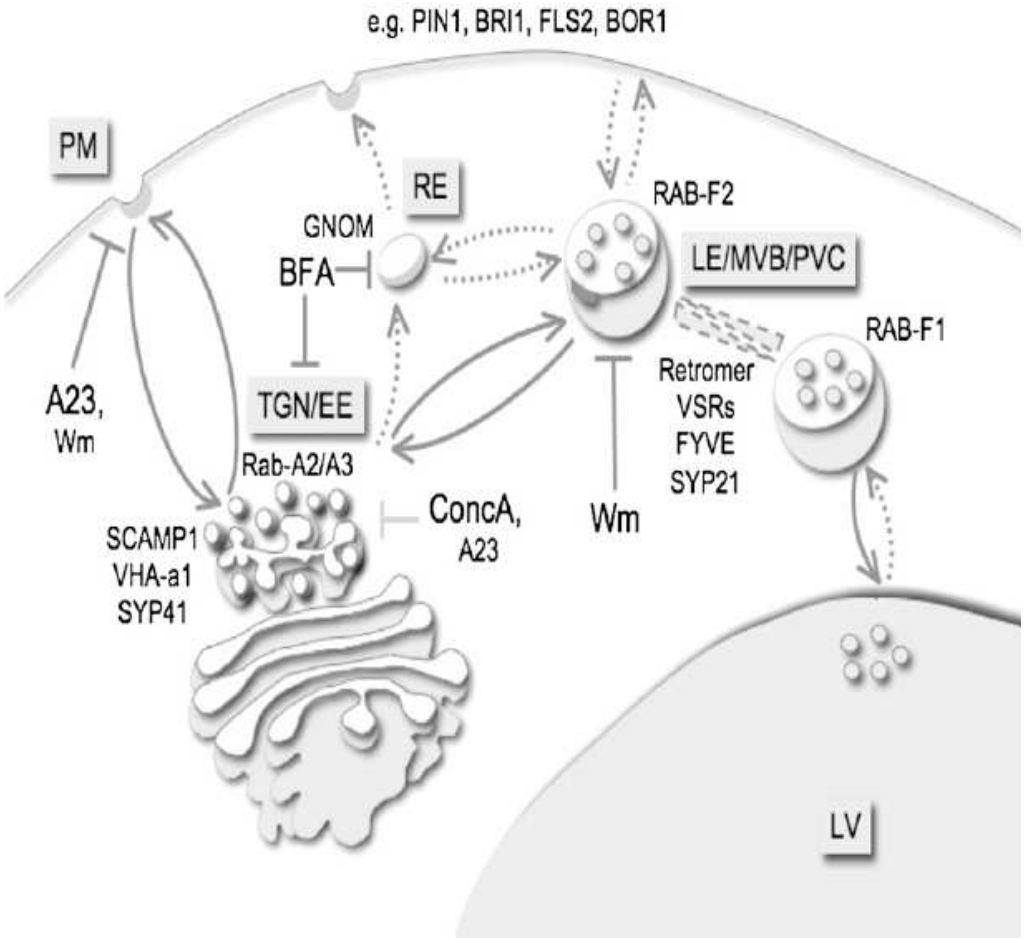

Endocytické váčky mají clathrinový obal

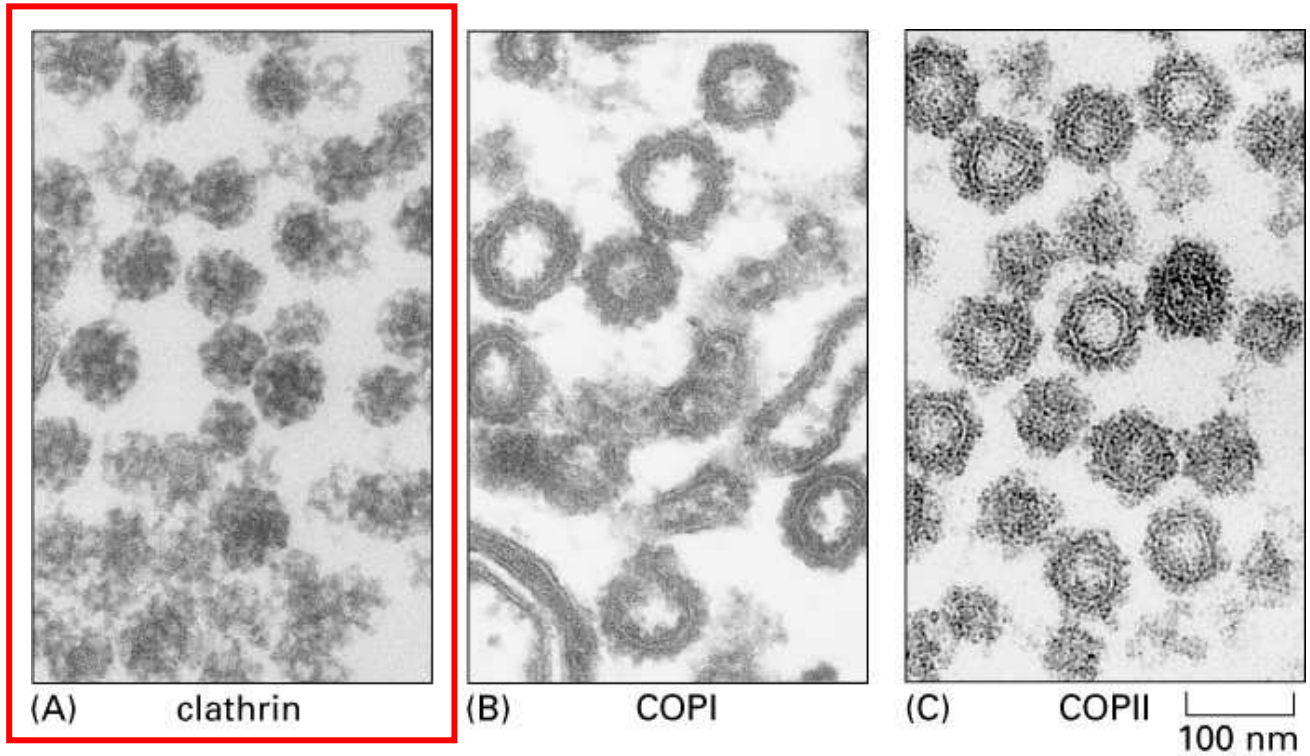

Various receptors and clathrin protein coats recognize vesicle types, and these are delivered (along cytoskeleton pathways?) to appropriate target sites in the cell.

Other recognition molecules, such as (vesicle) v-SNARE and (target) t-SNARE are involved in targeting vesicles with one set of contents to one site, and another set of vesicles to another site.

Genom Arabidopsis obsahuje celý komplement genů kódujících a regulujících klatrinové obaly.

TYPY ENDOCYTOTICKÝCH VÁČKŮ

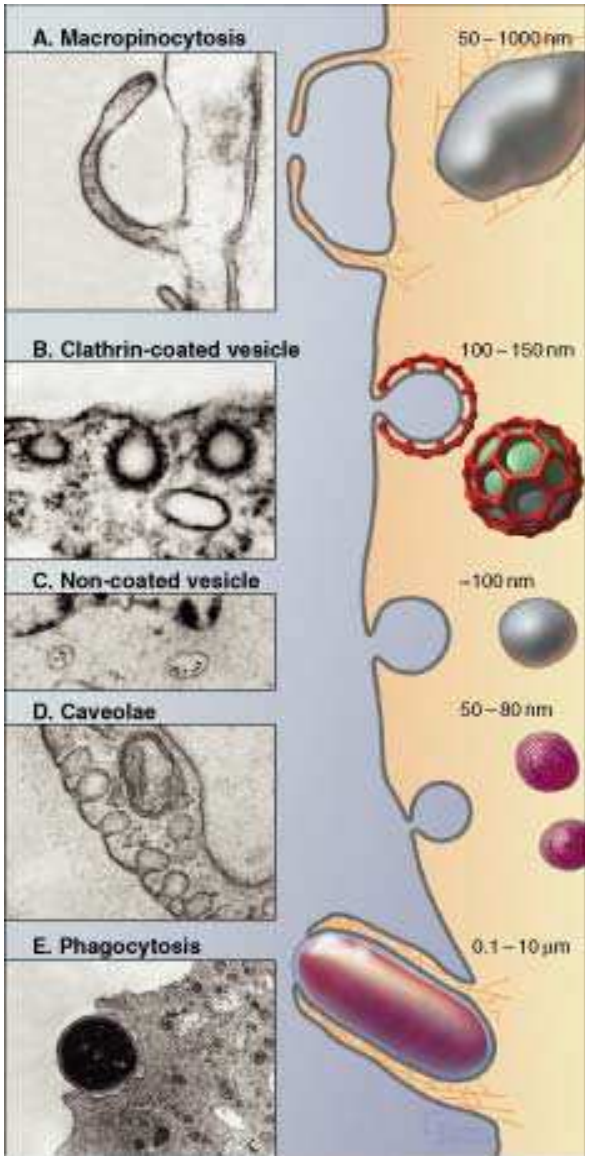

Endocytické váčky mají clathrinový obal

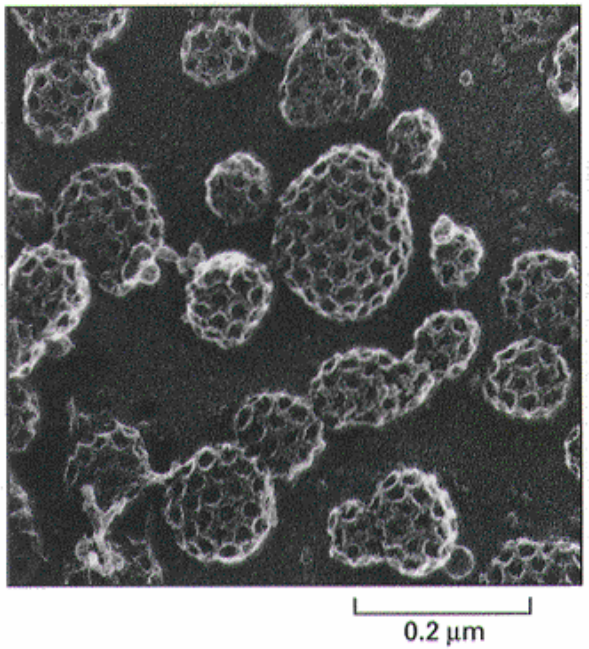

Figure 13-6. Clathrin-coated pits and vesicles. This rapid-freeze, deep-etch electron micrograph shows numerous clathrin-coated pits and vesicles on the inner surface of the plasma membrane of cultured fibroblasts. The cells were rapidly frozen in liquid helium, fractured, and deep-etched to expose the cytoplasmic surface of the plasma membrane. (From J. Heuser, *J. Cell Biol.* 84:560583, 1980. © The Rockefeller University Press.)

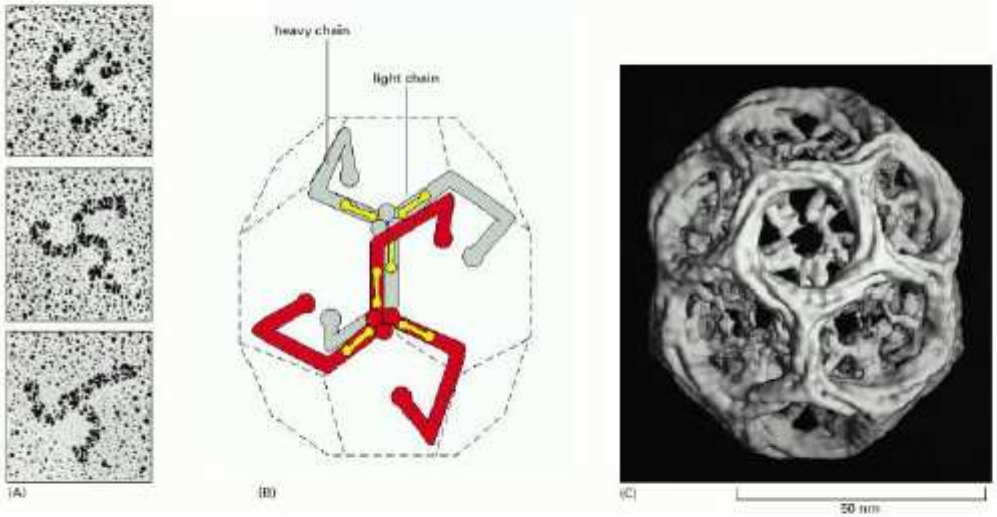

Figure 13-7. The structure of a clathrin coat. (A) Electron micrographs of clathrin triskelions shadowed with platinum. Although this feature cannot be seen in these micrographs, each triskelion is composed of 3 clathrin heavy chains and 3 clathrin light chains. (B) A schematic drawing of the probable arrangement of triskelions on the cytosolic surface of a clathrin-coated vesicle. Two triskelions are shown, with the heavy chains of one in *red* and those of the other in *gray*; the light chains are shown in *yellow*. The overlapping arrangement of the flexible triskelion arms provides both mechanical strength and flexibility. Note that the end of each leg of the triskelion turns inward, so that its N-terminal domain forms an intermediate shell. (C) A cryo electron micrograph taken of a clathrin coat composed of 36 triskelions organized in a network of 12 pentagons and 6 hexagons. The interwoven legs of the clathrin triskelions form an outer shell into which the N-terminal domains of the triskelions protrude to form an inner layer visible through the openings. It is this inner layer that contacts the adaptor proteins (adaptins) shown in the next figure. Although the coat shown is too small to enclose a membrane vesicle, the clathrin coats on vesicles are constructed in a similar way from 12 pentagons plus a larger number of hexagons, resembling the architecture of a soccer ball. (A, from E. Ungewickell and D. Branton, *Nature* 289:420422, 1981. © Macmillan Magazines Ltd.; B, from I.S. Nathke et al., *Cell* 68:899910, 1992. © Elsevier; C, courtesy of B.M.F. Pearse, from C.J. Smith et al., *EMBO J.* 17:49434953, 1998.)

Clathrin coated vesicles. Deep freeze etching EM of inner surface of plasma membrane of cultured fibroblast cells.

Tvorba endocytických váčků

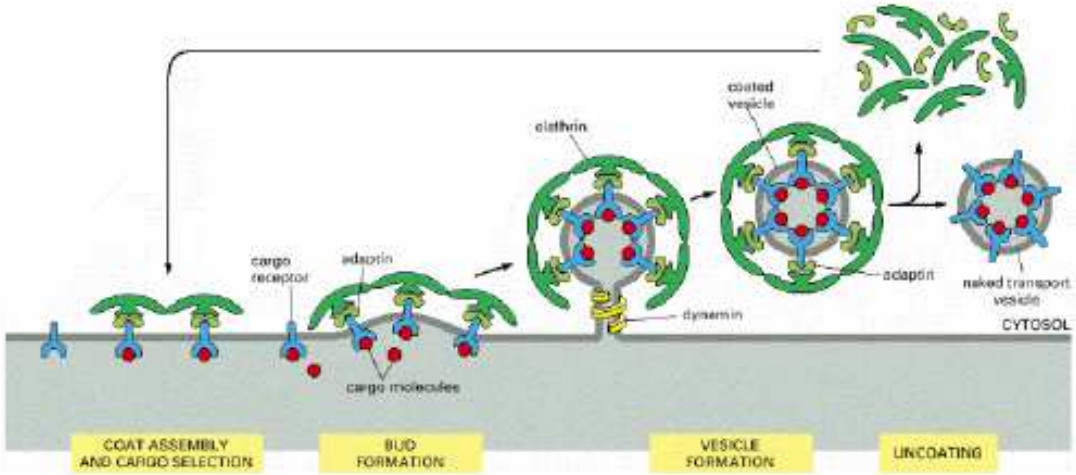

Figure 13-8. The assembly and disassembly of a clathrin coat. The assembly of the coat is thought to introduce curvature into the membrane, which leads in turn to the formation of uniformly sized coated buds. The adaptins bind both clathrin triskelions and membrane-bound cargo receptors, thereby mediating the selective recruitment of both membrane and cargo molecules into the vesicle. The pinching-off of the bud to form a vesicle involves membrane fusion; this is helped by the GTP-binding protein dynamin, which assembles around the neck of the bud. The coat of clathrin-coated vesicles is rapidly removed shortly after the vesicle forms.

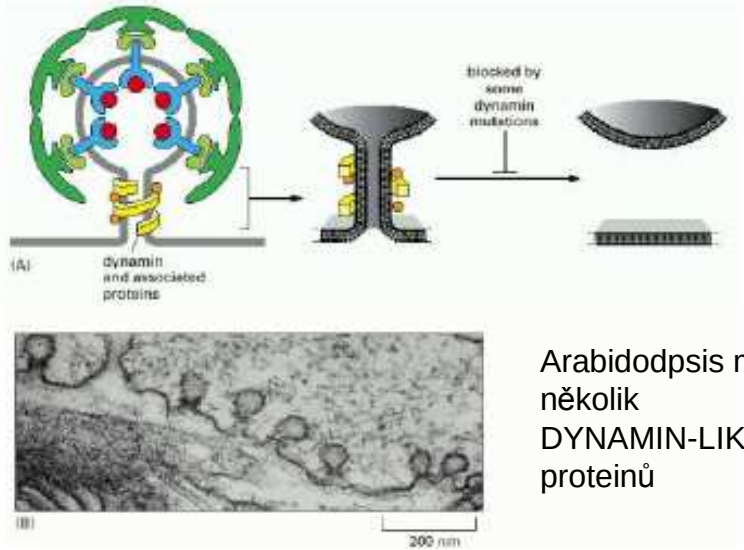

Arabidodpsis má několik DYNAMIN-LIKE proteinů

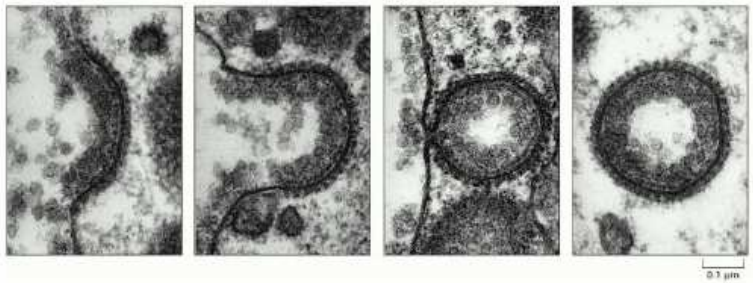

Figure 13-41. The formation of clathrin-coated vesicles from the plasma membrane. These electron micrographs illustrate the probable sequence of events in the formation of a clathrin-coated vesicle from a clathrin-coated pit. The clathrin-coated pits and vesicles shown are larger than those seen in normal-sized cells. They are involved in taking up lipoprotein particles into a very large hen oocyte to form yolk. The lipoprotein particles bound to their membrane-bound receptors can be seen as a dense, fuzzy layer on the extracellular surface of the plasma membrane - which is the inside surface of the vesicle. (Courtesy of M.M. Perry and A.B. Gilbert, *J. Cell Sci.* 39:257272, 1979. © The Company of Biologists.)


α chain
μ chain

adaptiny

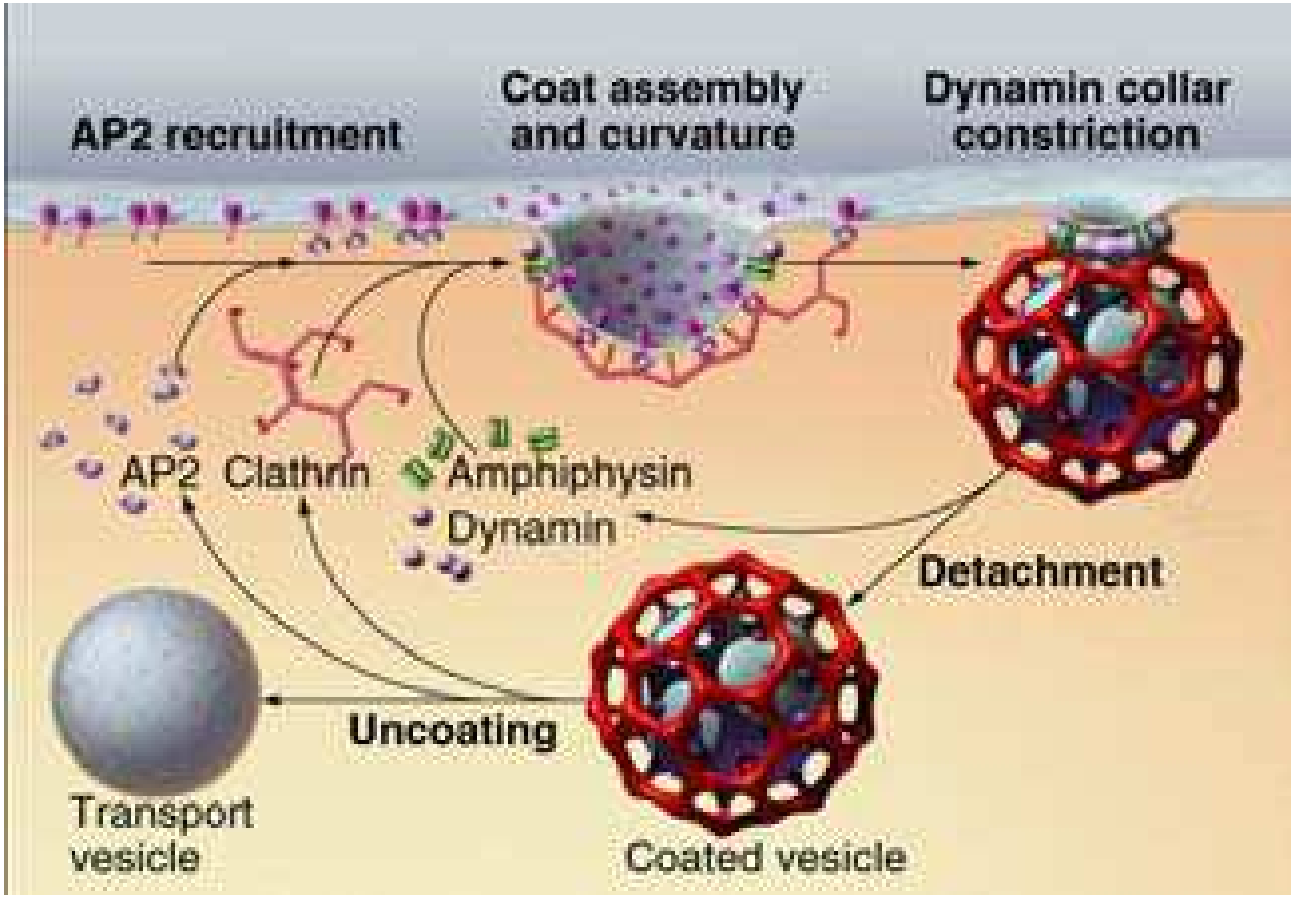
AP2 recruitment
Coat assembly and curvature
Dynamin collar constriction
AP2
Clathrin
Amphiphysin
Dynamin
Detachment
Uncoating
Transport vesicle
Coated vesicle

- Bin–Amphiphysin–Rvs (**BAR**) domain proteins, which can sense membrane curvature and recruit actin to membranes. BAR proteins interact with the endocytic and cytoskeletal machinery, including the GTPase dynamin (which mediates vesicle fission), N-WASP (an Arp2/3 complex regulator) and synaptojanin (a phosphoinositide phosphatase).

Tvorba endocytických váčků

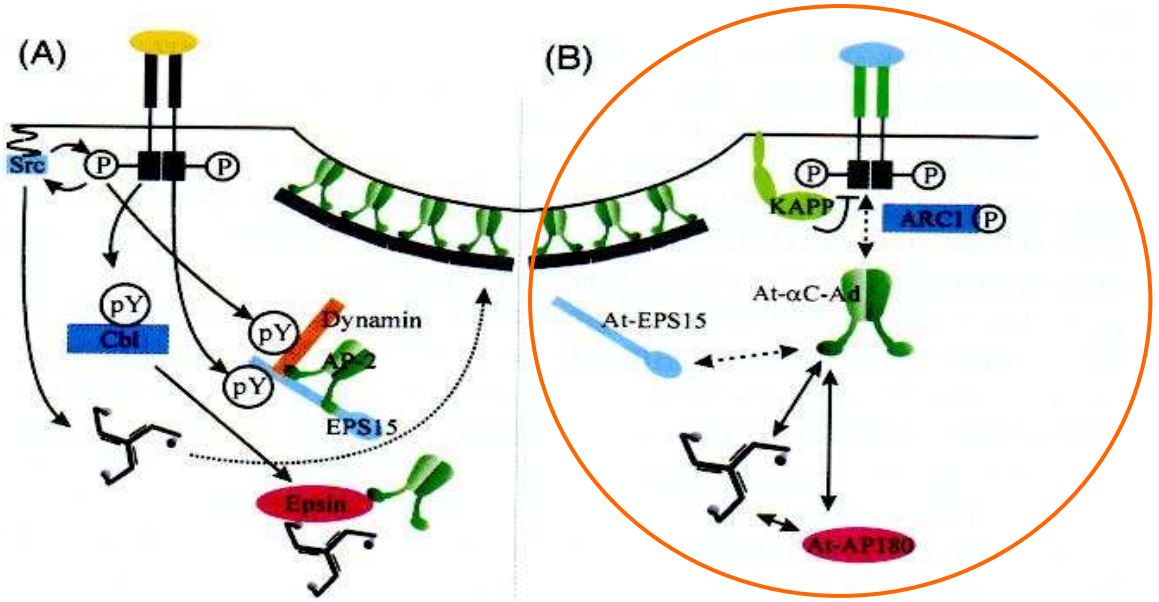

Fig. 1 Model depicting established and putative interactions of mammalian receptor protein kinases (RPKs) and plant receptor-like kinases (RLK) with components of the clathrin endocytosis machinery. **A** Binding of its ligand EGF induces the dimerization of the RPK EGF-R and also its trans-autophosphorylation on tyrosine residues located within its cytoplasmic domain. These in turn represent docking sites for SH2- or phosphotyrosine binding domain containing downstream effector proteins such as the ubiquitin ligase c-Cbl and EPS15, which assemble a signalling network for the regulation of the intracellular response to the ligand. In addition, the EGF-R itself is an active cargo since it modifies directly components of the clathrin endocytosis machinery by covalently phosphorylating their tyrosine residues. **B** The hypothetical model of plant RLK internalization shows similarities to the down-regulation of mammalian RPKs. Plant RLKs also dimerize after ligand binding and some contain the YXXϕ-internalization motif while others might be prone to ubiquitylation. Furthermore, dephosphorylation by the plant-specific phosphatase KAPP is also crucial for their internalization. Several plant homologs of the clathrin endocytosis machinery, required for the downregulation of signalling receptors, have been functionally characterized and their interactions are demonstrated by *solid arrows* (see text) while putative interactions are indicated by *dashed arrows*. An EPS15 homolog has been identified from the *Arabidopsis* database (Holstein 2002)

Aktivovaný receptor (např. receptorová kináza) může stabilizovat vznikající „obalené jámy“.

Signální/signalizační endosom

Internalizace obsazeného receptoru (recyklace) nemusí být jen krok vedoucí k oslabení signalizace jeho destrukcí, ale v některých případech signalizace pokračuje v endosomu – tzv. signalizační endosom (např. signalizace brassinosteroidy – BRI1).

Regulace pomocí Rab GTPáz

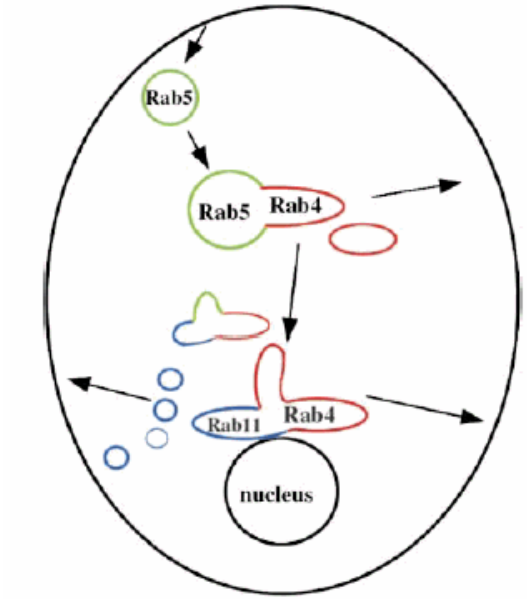

organely spojené s endocytózou jsou mozaikou membránových domén

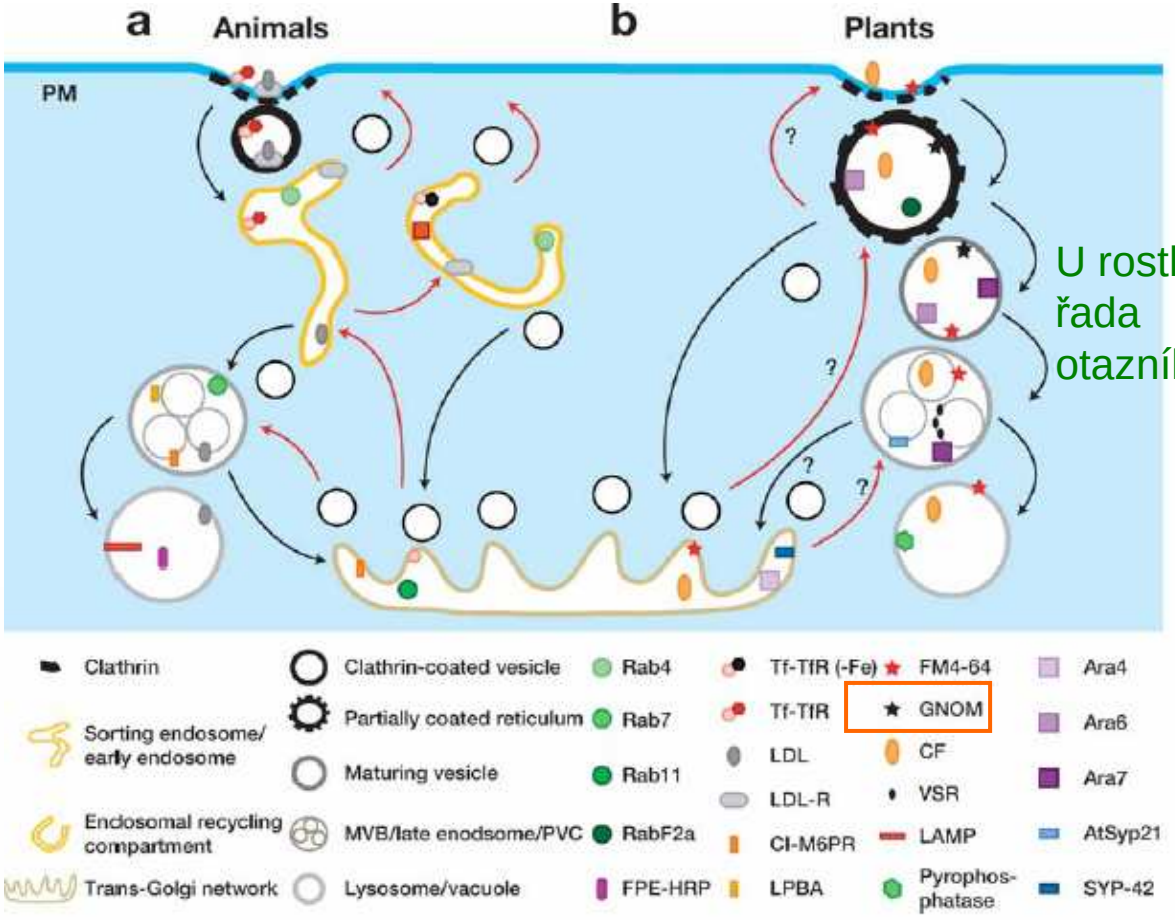

U rostlin řada otazníků!

Endocytotic cycling in animals and plants. Endocytotic cycling is well studied in animal cells with several types of cycling known: clathrin-mediated, clathrin-coated receptor-mediated, nonclathrin-mediated (caveolae/lipid raft–mediated, fluid-phase endocytosis, phagocytosis). In contrast, little is known about endocytosis in plants and much has been extrapolated from animal literature. Two discrete endosomal compartments have been identified in plants, as well as a gradation of maturation from one to the other. Redirection of endocytosed PM proteins back to the PM has not been directly demonstrated but is strongly supported by indirect evidence (43, 44). Black arrows indicate the endocytotic pathway; red arrows indicate the secretory pathway. (*A*) In animals, clathrin-coated and receptor-mediated endocytosed vesicles from the plasma membrane (PM) are directed to the sorting endosome/early endosome [Rab4, LDL-receptor (LDL-R) and transferrin receptor (TfR) markers]. From there, cargo is transported to the PM, endosomal recycling compartment [Rab4, Rab11, LDL-R, transferrin bound to transferrin receptor (Tf-TfR)], or multivesicular body (MVB)/late endosome [Rab7, M6PR, lysobisphosphatidic acid (LPBA) (87)]. From the endosomal recycling compartment, cargo can traffic back to the PM or the trans-Golgi network (TGN) (Rab11). From the MVB/late endosome, cargo can travel to the TGN [cationic-independent mannose-6-phosphate receptor (CI-M6PR)] or the lysosome [fluid-phase endocytosed HRP (FPE-HRP), lysosome-associated membrane protein (LAMP) (24)]. Cargo can also travel from the TGN to the sorting endosome/early endosome and MVB/late endosome. (*B*) In plants, cargo and PM proteins/markers are endocytosed into the partially coated reticulum (PCR) [catonized ferritin (CF), GNOM, Ara6, FM4-64, RabF2a]. From the PCR, vesicle maturation results in direction of cargo to MVBs [CF, FM4-64, Ara7, AtSyp21, VSR proteins] through vesicle maturation with overlapping compartment markers [Ara6 and Ara7] or the TGN [CF, FM4-64, SYP-42, Ara4]. From the MVB/late endosome/prevacuolar compartment (PVC), cargo is trafficked to the vacuole [CF, FM4-64, pyrophosphatase (139)]; trafficking to the TGN is hypothesized. Trafficking from the TGN to the PCR or MVB has not been demonstrated.

Endocytóza

Při endocytóze PM velmi pravděpodobně může také docházet k internalizaci (modifikaci a posléze recyklaci) části pektinů a xyloglukanů buněčné stěny.

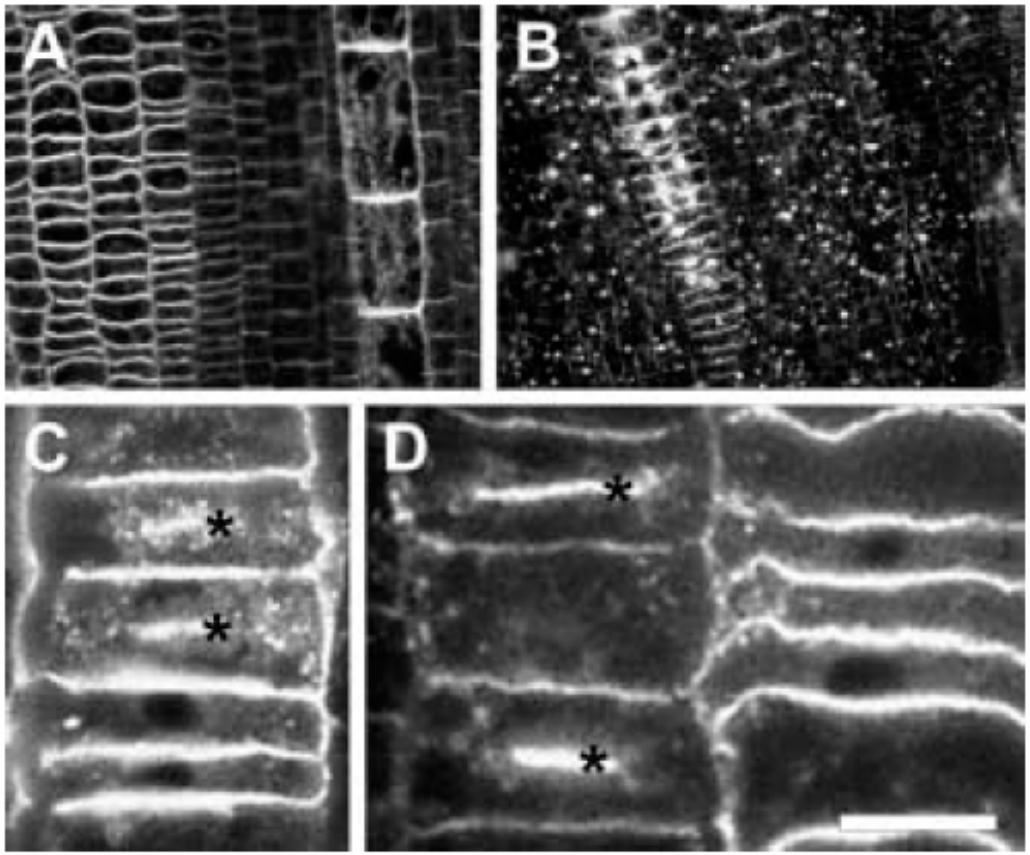

Po přidání BFA (B) jsou téměř všechny xyloglukany internalizovány do BFA kompartmentu.

Fig. 7A–C. A Xyloglucans are very abundant in cross walls of xylem elements and of cells in the middle and outer cortex. B In BFA-treated cells, almost all xyloglucans internalize into abundant BFA compartments. C and D In cytokinetic cells, xyloglucans are localized within compartments sized between about 500 and 1000 nm, which by their fusion build both the early and late cell plates. Bar: 15 μm

Markery endocytózy

FM styrylové sloučeniny/barvičky fluoreskují po zapojení do membrány.
Internalizují se endocyózou.
Optimální pro rostlinné buňky je FM4-64

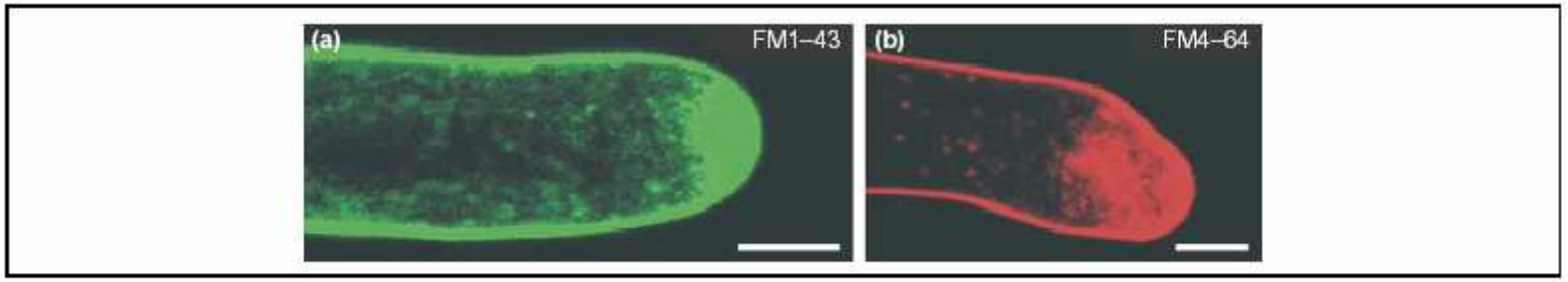

Figure 1. Integrated endocytic and secretory networks in tip-growing root hairs of plants. (**a,b**) Actively growing root hairs, like pollen tubes [35,71], internalize endocytic tracers FM1–43 (a) and FM4–64 (b) within minutes and accumulate them throughout their growing tips. Bars, 4 μm. Pictures courtesy of Miroslav Ovecka (University of Vienna, Austria).

pylové láčky lilie +
FM 4-64

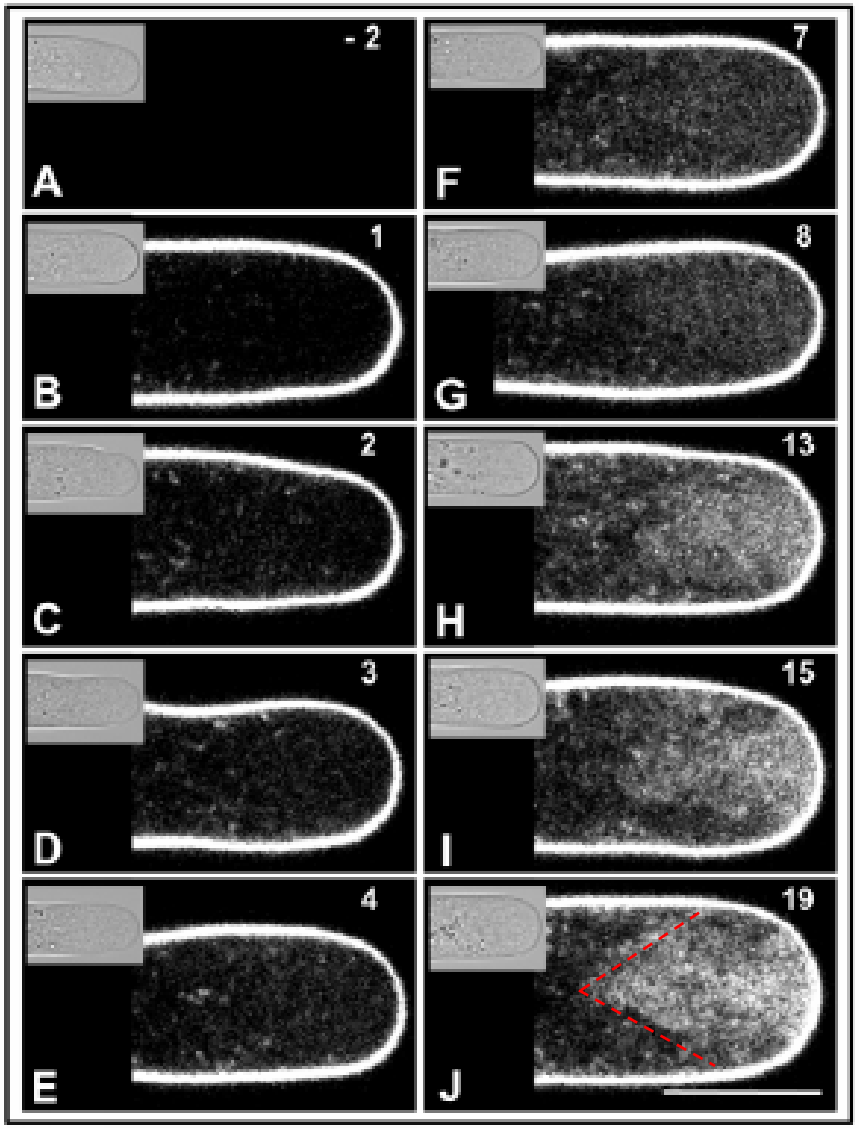

inverted cone

Fig. 4. FM4-64-uptake time course in a growing *L. longiflorum* pollen tube. (A-J) Median confocal fluorescence images at increasing times (minutes) after addition of FM4-64 (2 µM in 115% standard medium). To avoid osmotic perturbation, pollen tubes were pretreated with 115% medium before dye application. Inserts show bright field images at 1/3 size. Bar, 20 µm.

- V rostlinných buňkách hraje důležitou roli také endocytóza nezávislá na klathrinu.

Endosomy

Interakce GTPázy-lipidy

základní regulační smyčka endomembránového systému

- Lokální specifické domény membránových fosfolipidů jsou klíčovou součástí udržování identity nejen celých organel, ale také subdomén na organelách.

- Arf, Rho a Rab GTPázy regulují některé aktivity - kinázy, fosfolipázy, flipázy, které vytvářejí lokalizované membránové domény.

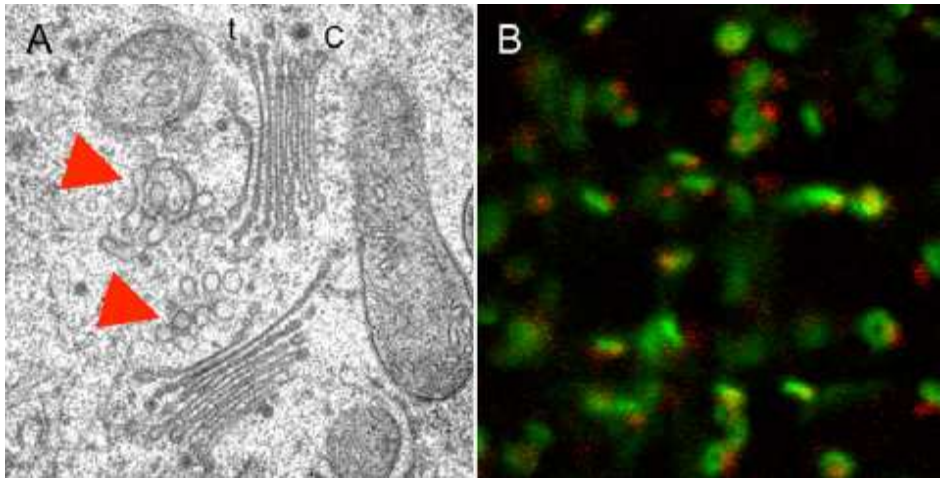

sialyl trasferáza
(trans-GA marker)

VHA-a1
(TGN marker)

Interakce GTPázy-lipidy

Rab GTPázy lze použít jako markery
různých součástí endomembránového systému

Table III. *Classification of endosomes*

Type	Lipid Markers	Rab Markers	pH	Other Markers
Sorting (early)	Structural sterols, PI-3-P	Rab5, Rab4	5,9–6,0	Annexin II
Recycling	Structural sterols	Rab4, Rab11	6,4–6,5	
Multivesicular body	PI-3-P		5,0–6,0	ESCRT, Hrs, Alix
Late	Lysobisphosphatidic acid	Rab7, Rab9	5,0–6,0	Alix
Lysosome/vacuole		Rab27A	5,0–5,5	

Interakce GTPázy-lipidy

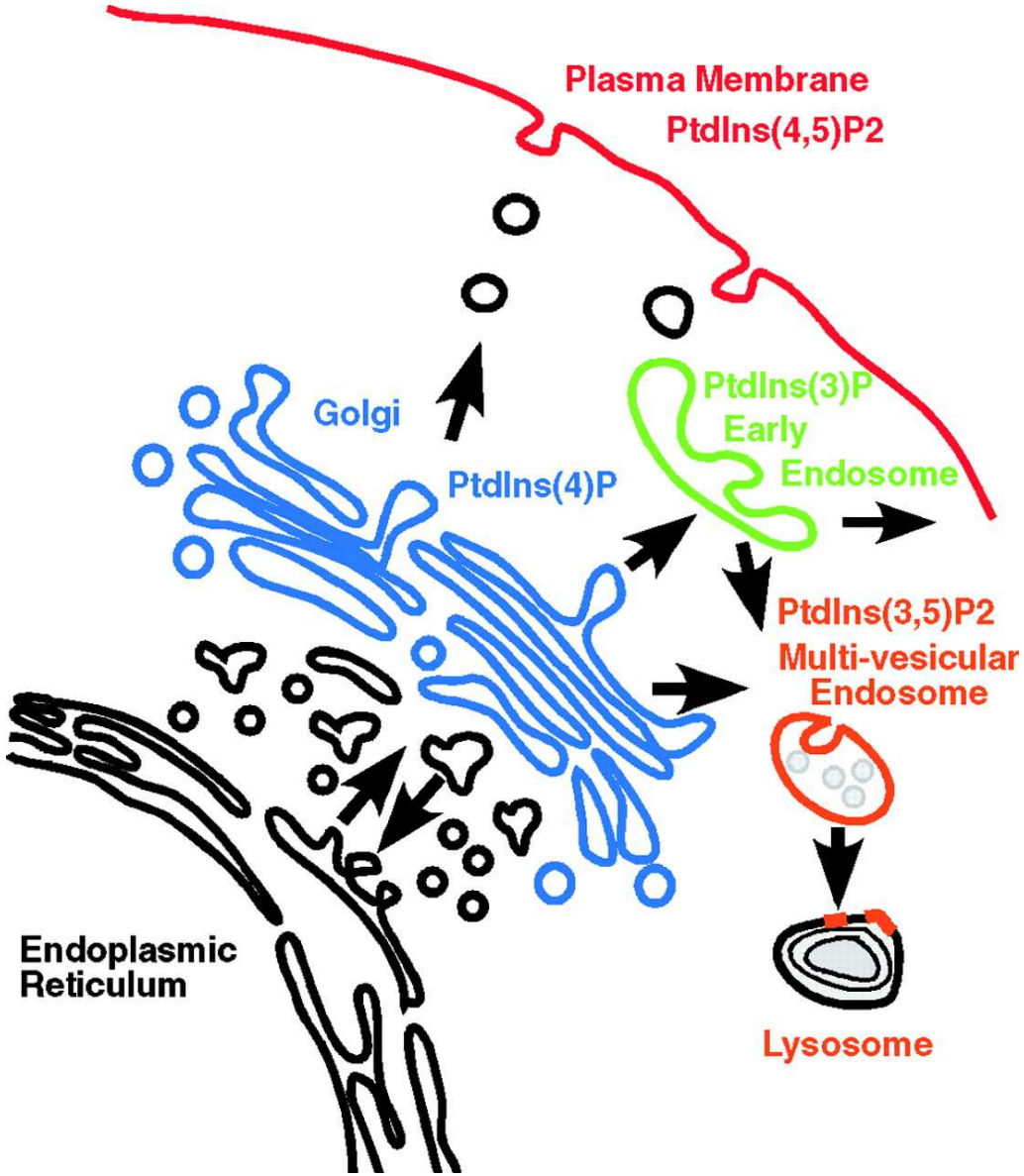

Distribution of phosphatidylinositides in cells:

PI(4)P (blue) - concentrated on Golgi

PI(3)P (green) - early endosomes

$PI(4,5)P_2$ - plasma membrane

$PI(3,5)P_2$ - multi-vesicular endosomes

Roth 2004

Structure of PI(3)P-binding modules

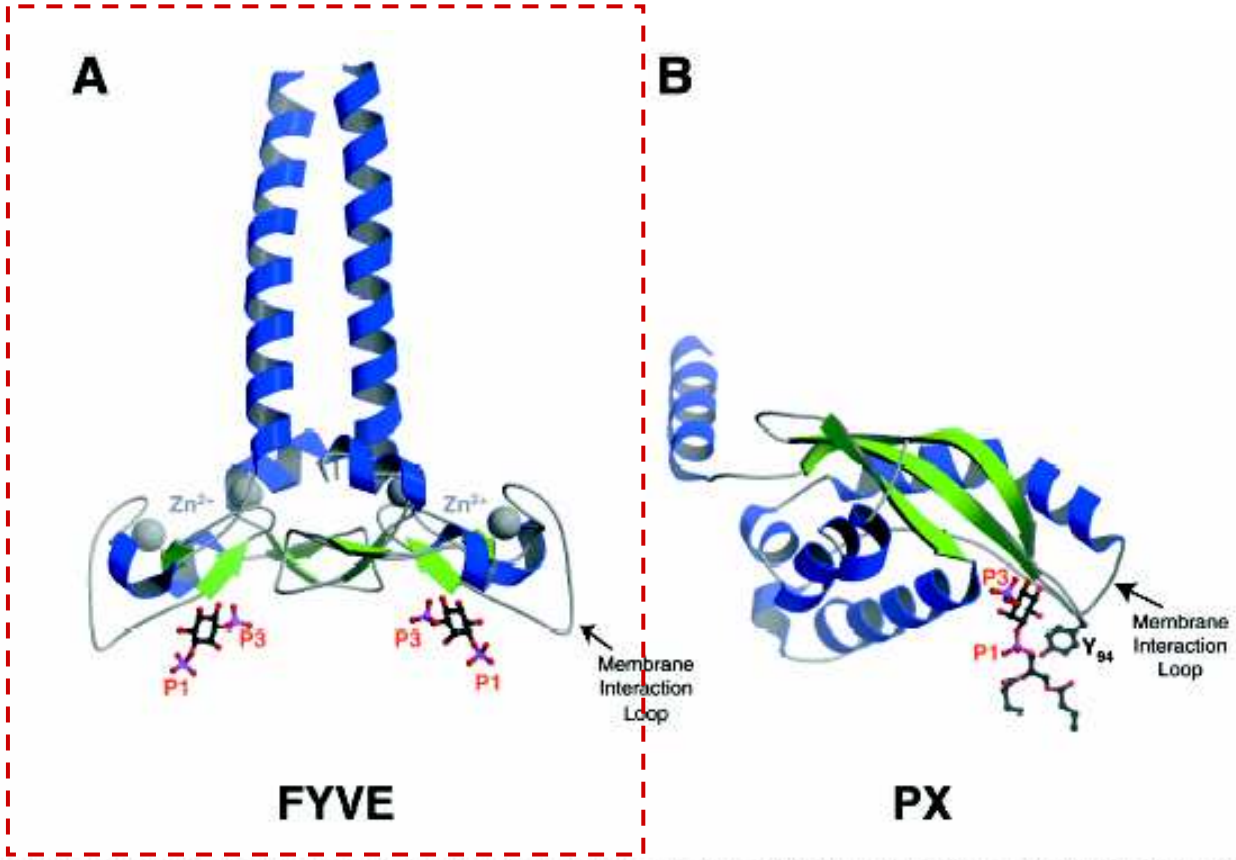

Figure3: Structures of (A) the EEA1 FYVE domain dimer (PDB code 1JOC) (31) and (B) the p40^{phox} PX domain (PDB code 1H6H) (30) bound to Ins(1,3)P_2 and dibutanoyl-PtdIns(3)P, respectively. The two domains are oriented such that the membrane in which the bound phosphoinositide would be embedded is perpendicular to the page, passing beneath the representation of the two domains. The 1-and 3-phosphates are labeled P1 and P3, respectively. Dimerization of the FYVE domain is driven by a 60 amino-acid N-terminal extension that forms a coiled-coil. In the FYVE domain, the two bound Zn^{2+} ions per protomer are colored gray. In the PX domain, the Y94 side-chain, which makes van der Waal's contact with the glycerol backbone is shown and labeled (see text). The loop labeled 'membrane interaction loop' is thought to insert into the membrane in both cases, based on NMR chemical shift changes seen upon binding of each domain to PtdIns(3)P-containing micelles (37,42).

Lemmon 2003

FYVE lze použít jako marker endosomů

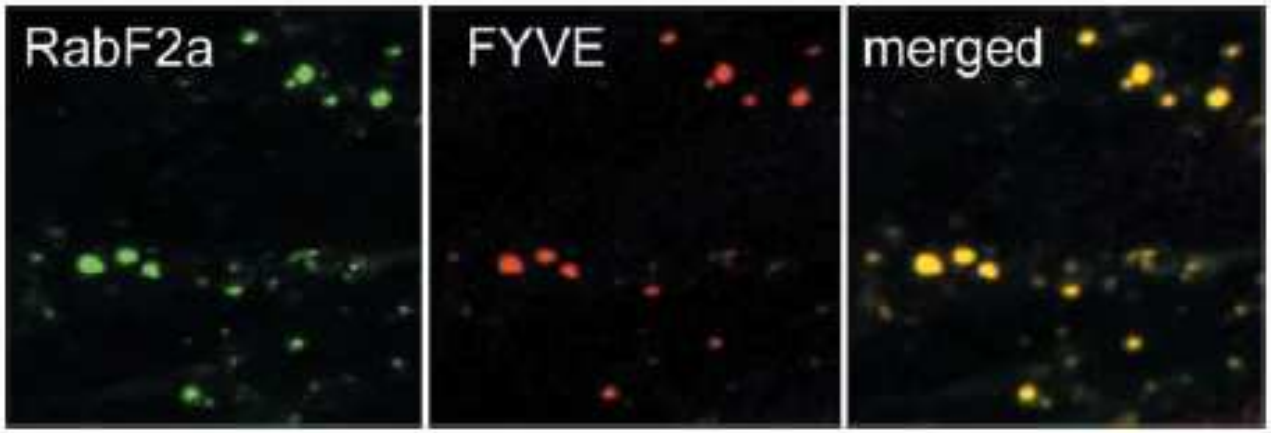

Plant Physiol. Vol. 135, 2004

Figure 1. Onion cells were cotransformed with two constructs: YFP-tagged RabF2a (shown in artificial green color) and DsRed-tagged double FYVE (shown in red). Pronounced colocalization of both constructs on endosomes (yellow) is shown in the merged image indicating that the double FYVE construct is a reliable endosomal marker in plant cells.

Lokalizace různých Rab GTPáz odhaluje různorodost endosomů

Distinct Localization of Ypt3/Rab11 in Higher Plants

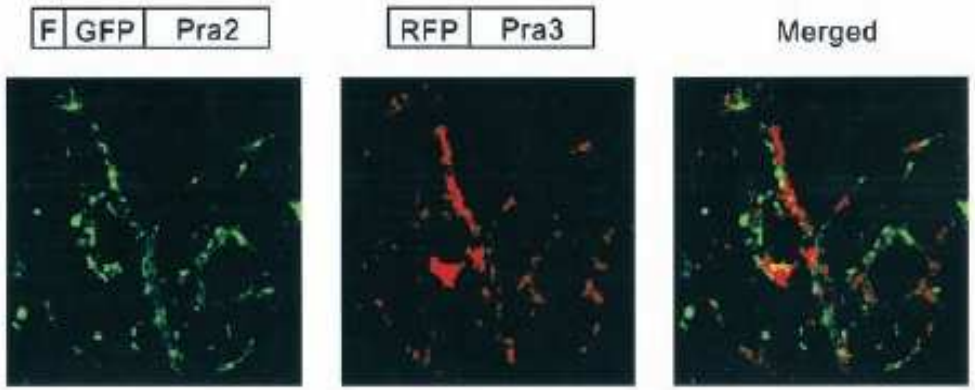

FIG. 7. **Distinct localization of Pra2 and Pra3 in tobacco BY-2 cells.** The plasmid carrying the *RFP-PRA3* fusion gene was intro
obacco cells expressing GFP-Pra2 by particle bombardment. After incubation for 18 h, cells were observed by a confocal laser-scanning n
, FLAG-tag.

Ara6, homolog Rab5 (RabF u At), je lokalizován SPÍŠE V POZDNÍM endosomu

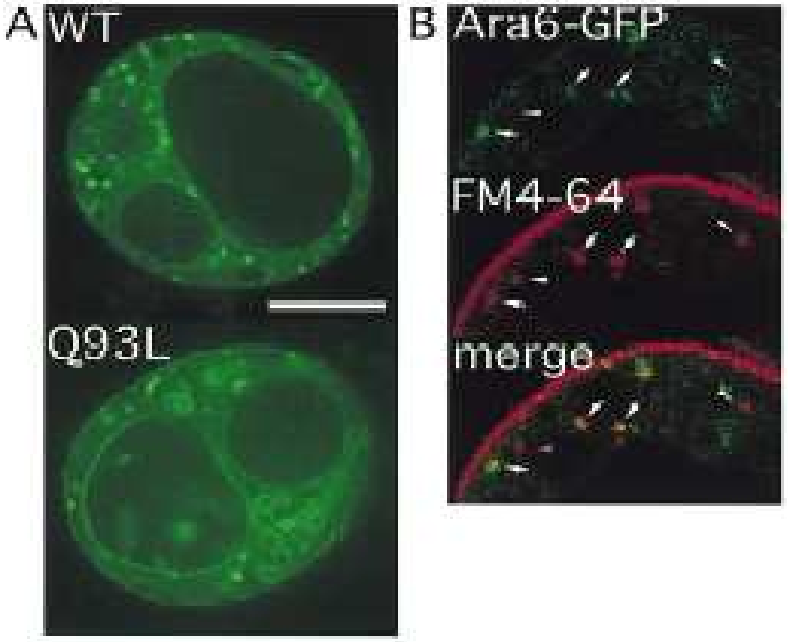

Fig. 3. Ara6, a plant-unique Rab GTPase, is localized on the subpopulation of early endosomes and regulates endosomal fusion. (A) $Ara6^{WT}$-GFP was distributed mainly on the early endosomes, and dominant active $Ara6^{Q93L}$-GFP was observed on aggregating vesicles and vacuoles. (B) Protoplasts of suspension-cultured *Arabidopsis* cells expressing $Ara6^{WT}$-GFP were labeled by FM4-64, a tracer of the endocytic pathway. The dots labeled by $Ara6^{WT}$-GFP (arrows) were also labeled by FM4-64. Note that some dots labeled by FM4-64 were not labeled by $Ara6^{WT}$-GFP (arrowheads). Bar = 10 μm.

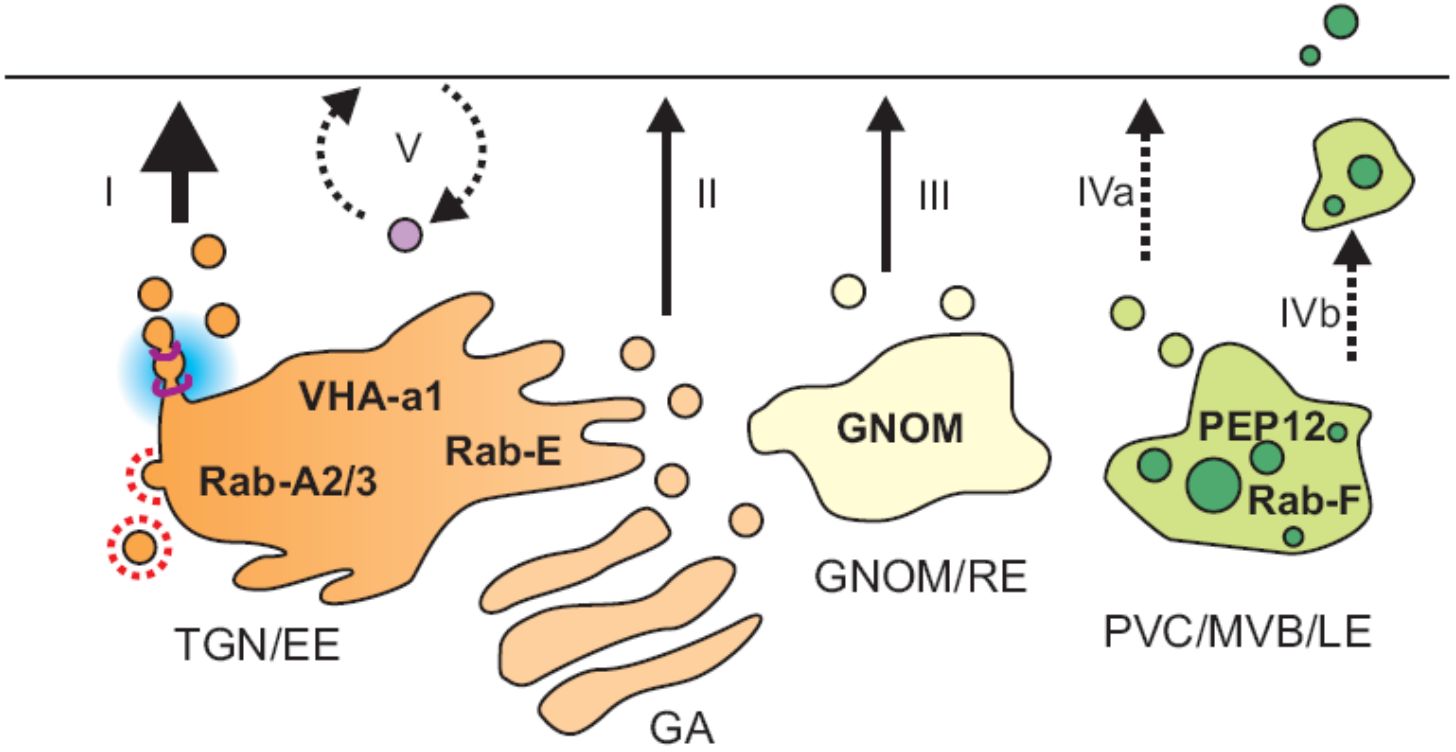
I
V
II
III
IVa
IVb
VHA-a1
Rab-E
Rab-A2/3
GNOM
PEP12
Rab-F
TGN/EE
GA
GNOM/RE
PVC/MVB/LE

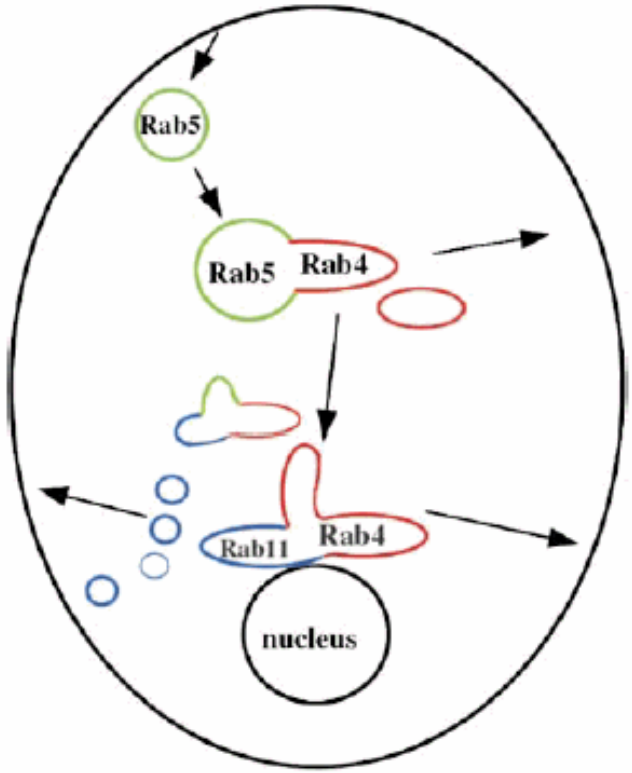

Figure 7. Model, describing endocytic organelles as a mosaic of membrane domains. The domain distribution of the three Rab proteins presented in this study, Rab4, Rab5, and Rab11 is depicted in red, green, and blue, respectively. Compartmentalization is achieved by dynamic functional arrangements of these domains, combinations of Rab4 and Rab5, and Rab4 and Rab11 being the most abundant. Arrows indicate direction of transferrin recycling. Cargo enters the cell via mainly Rab5-containing structures. Fast recycling is achieved by rapid sorting from Rab5 into Rab4-positive domains on the same endosome. Recycling slows down once transferrin enters pericentriolar membranes dominated by Rab4 and Rab11 domains.

Recyklace plasmatické membrány

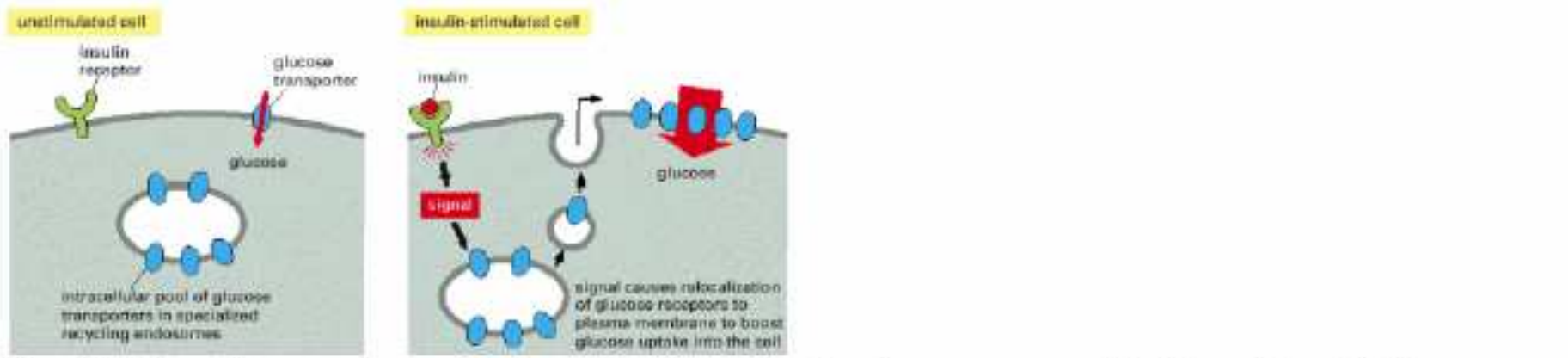

Figure 13-52. Storage of plasma membrane proteins in recycling endosomes. Recycling endosomes can serve as an intracellular pool for specialized plasma membrane proteins, enabling them to be mobilized when needed. In the example shown here, insulin binding to the insulin receptor triggers a signaling pathway that causes the rapid insertion of glucose transporters into the plasma membrane of a fat or muscle cell, greatly increasing glucose intake.

Podobně je zřejmě regulována lokalizace auxinových přenašečů PIN. **Auxin blokuje endocytózu,** a tak automaticky zvyšuje výskyt výtokových přenašečů na PM. Takto auxin pravděpodobně reguluje svůj vlastní transport.

Pohyb endosomů

Endosomy se pohybují **po aktinových vláknech**, ale také mechanismem **aktinové komety**.
Pohyb je závislý na polymeraci aktinu a nezávislý na myosinu.

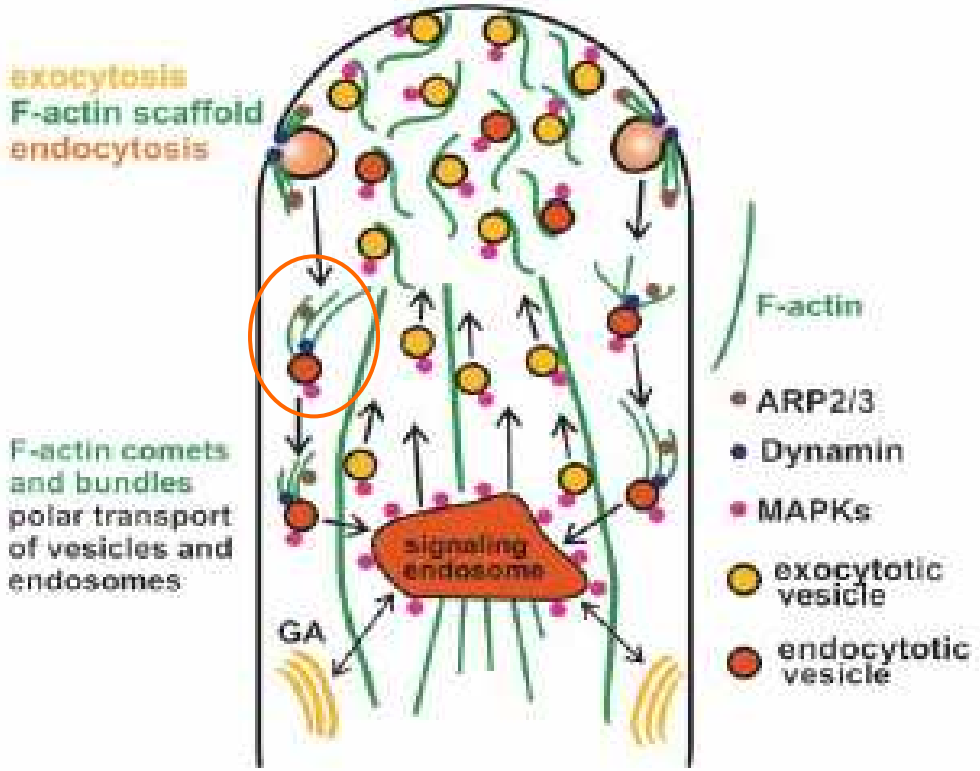

Figure 3. Working model depicting endosomal/vesicular trafficking and possible roles of the actin filaments in an idealized tip-growing root hair. Local actin polymerization together with accumulation of dynamin could facilitate endocytic recycling of receptors, ion channels, and cell wall molecules (e.g. pectins and AGPs) by assisting the pinching off the endocytic vesicles and by forming actin comets on these vesicles dependent on ARPs. Signaling molecules such as MAPKs associate both with endosomal vesicles and the actin cytoskeleton. Additionally, dense meshworks of actin filaments regulated by profilins and ARPs are suggested to act as a structural scaffold in order to sequester and maintain signaling and regulatory molecules, including MAPKs within the apical vesicle pool (clear zone). GA, Golgi apparatus. Arrows indicate polar trafficking of exo- and endocytic vesicles/endosomes, as well as putative transport between TGN and endosomes.

Brefeldin A (BFA)

BFA, inhibitor GEF pro Arf GTPázy, je důležitým nástrojem studia sekreční dráhy. Vede ke vzniku tzv. BFA kompartment.

Pozor, ne každý Afr GEF je citlivý k BFA! (Buňky Arabidopsis mají 8 GEFů pro 12 ARFů, různě silně exprimovaných a různě lokalizovaných.)

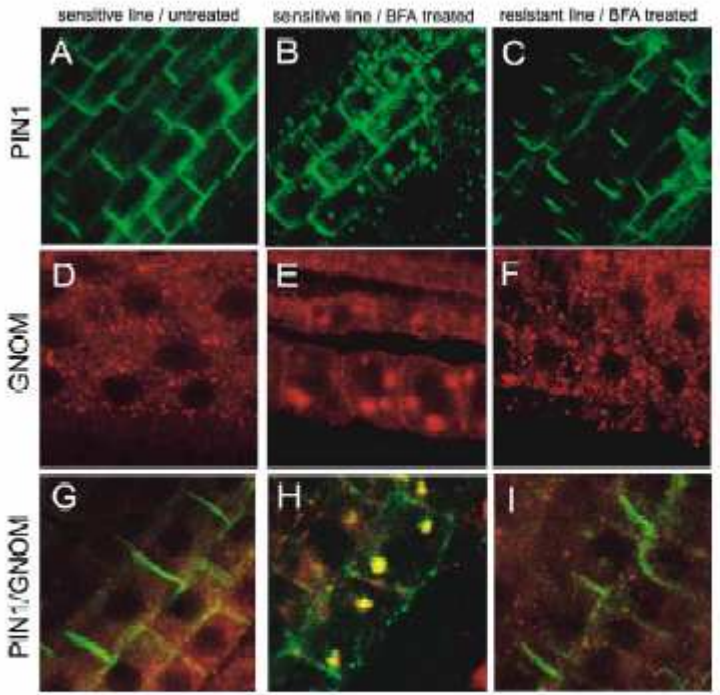

linie C, F, I jsou rezistentní k BFA

Figure 2. Brefeldin A Responses of PIN1 and GNOM Are Altered in Engineered GNOM Lines

Confocal images of seedling root tips stained with PIN1 antibody (green) and monoclonal myc antibody (red) on GNOM-myc transgenic lines. (A–C) PIN1, (D–F) GNOM-myc, and (G–I) PIN1 and GNOM-myc. (A, D, and G) Control treatment on GN^{wt}-myc line, (B, E, and H) BFA 50 μM for 60 min on GN^{wt}-myc line, and (C, F, and I) BFA 50 μM 60 min on GN^{5000}-myc line. Note yellow intracellular dots in (H), indicating colocalization of PIN1 and GNOM.

brefeldin A

Molecular Formula: $C_{16}H_{24}O_4$

Molecular Weight: 280.36

CAS Number/Name: 20350-15-6 / 1,6,7,8,9,11a,12,13,14,14a-Decahydro-1,13-dihydroxy-6-methyl-4H-cyclopent[f]oxacyclotridecin-4-one

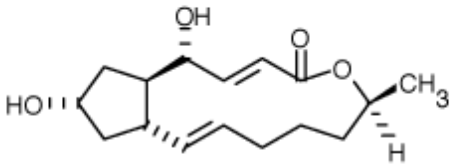

Polární transport auxinu (IAA) je závislý na polární lokalizaci PIN auxinových výtokových přenašečů. Jejich lokalizace je závislá na polarizované sekreci a aktinovém cytoskeletu.

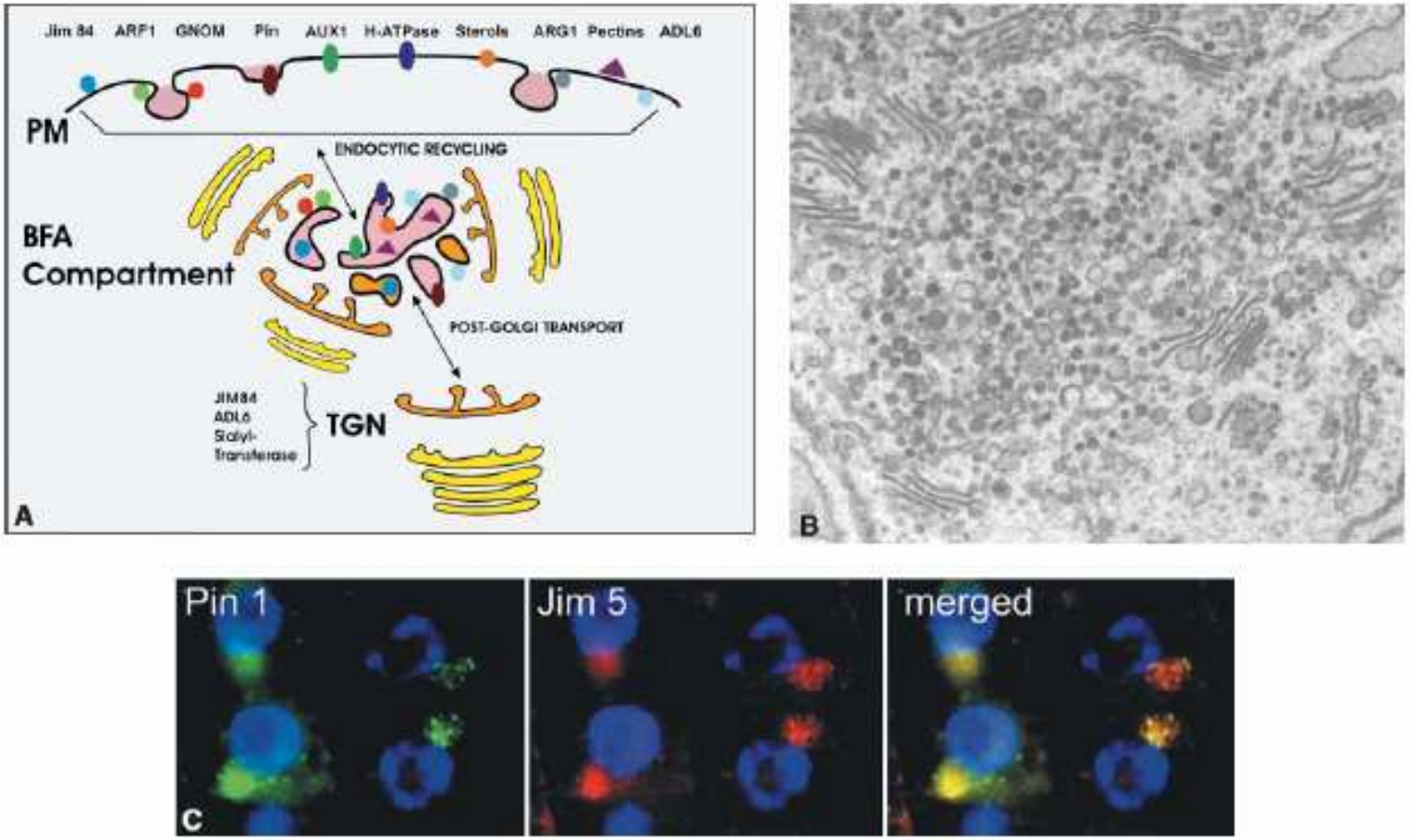

Figure 2. A, Endocytosis in plants—insights from BFA compartments. Upon BFA treatment, the following plasma membrane and plasma membrane-associated molecules accumulate in BFA compartments: PINs (putative auxin efflux carriers), AUX1 (putative auxin influx carrier), plasma membrane H-ATPase, plasma membrane structural sterols, and peripheral membrane protein ARG1 (altered response to gravity). Except this, cell wall pectins cross-linked by boron, small GTPase ARF1, and ARF activator GNOM (ARF-GEF) accumulate within BFA compartments. The JIM84 carbohydrate epitope and dynamin ADL6 associate both with plasma membrane and TGN, and can be eventually transported to the BFA compartment from both locations. Internalization of cell wall pectins could be inhibited by short-term boron deprivation. AUX1 accumulation to BFA compartments is restricted to protophloem cells. B, Ultrastructure of BFA compartment after 30-min incubation of root epidermal cell with 25 μM BFA (reproduced with permission from Grebe et al., 2003). C, Immunofluorescence colocalization of putative auxin efflux carrier PIN1 (second antibody coupled to FITC; green) and cell wall pectins recognized by monoclonal antibody JIM5 (secondary antibody coupled to TRITC; red) on BFA compartments (yellow) in maize root cells treated with 100 μM BFA for 2 h. Nuclei (blue) are counterstained with DAPI.

Endocytóza během cytokineze

Uspořádání mikrotubulů během buněčného cyklu rostlinné buňky

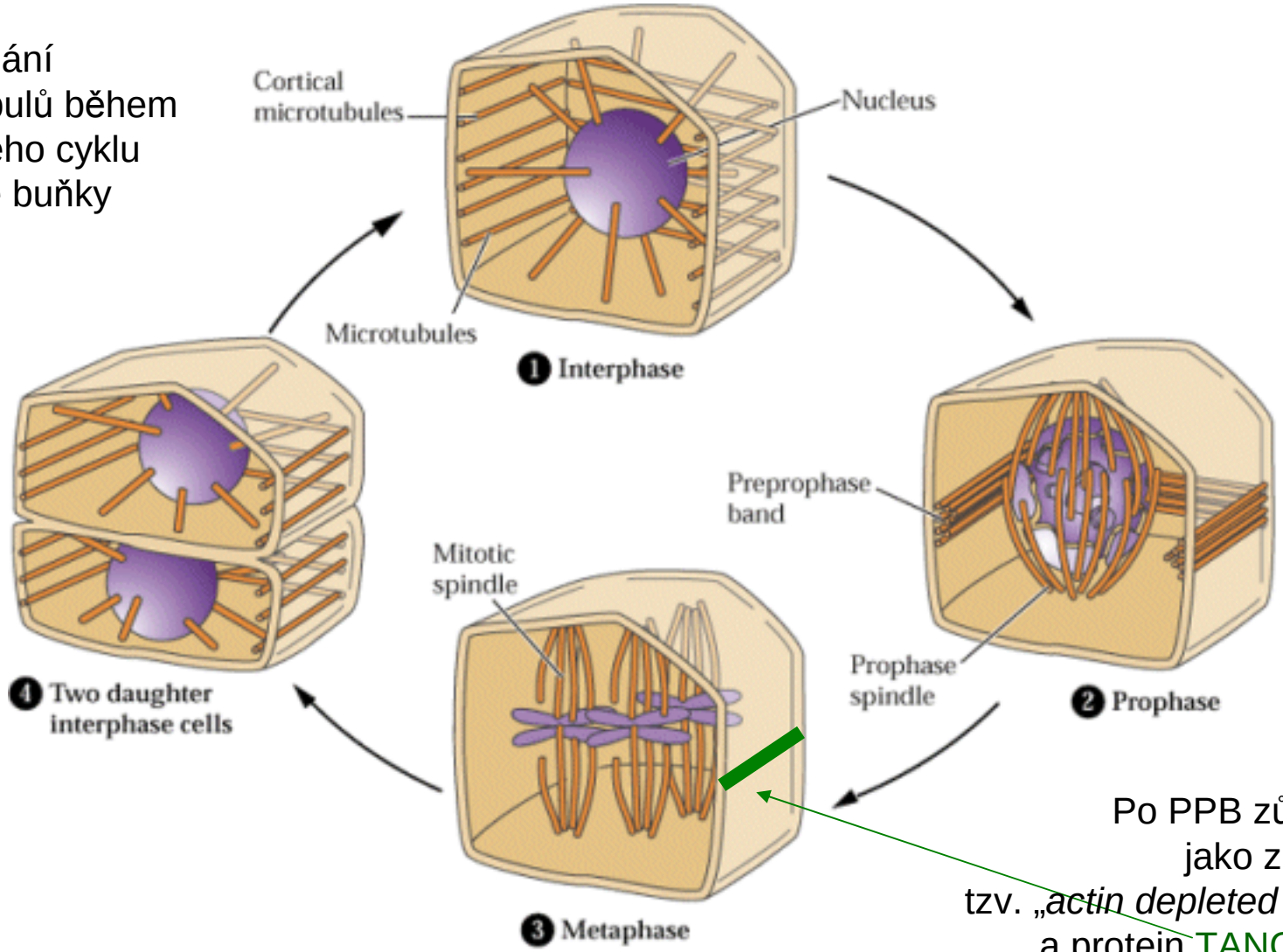

Po PPB zůstává jako značka tzv. „*actin depleted zone*“ a protein TANGLED.

Je rozdíl mezi rostlinami a živočichy opravdu tak zásadní?

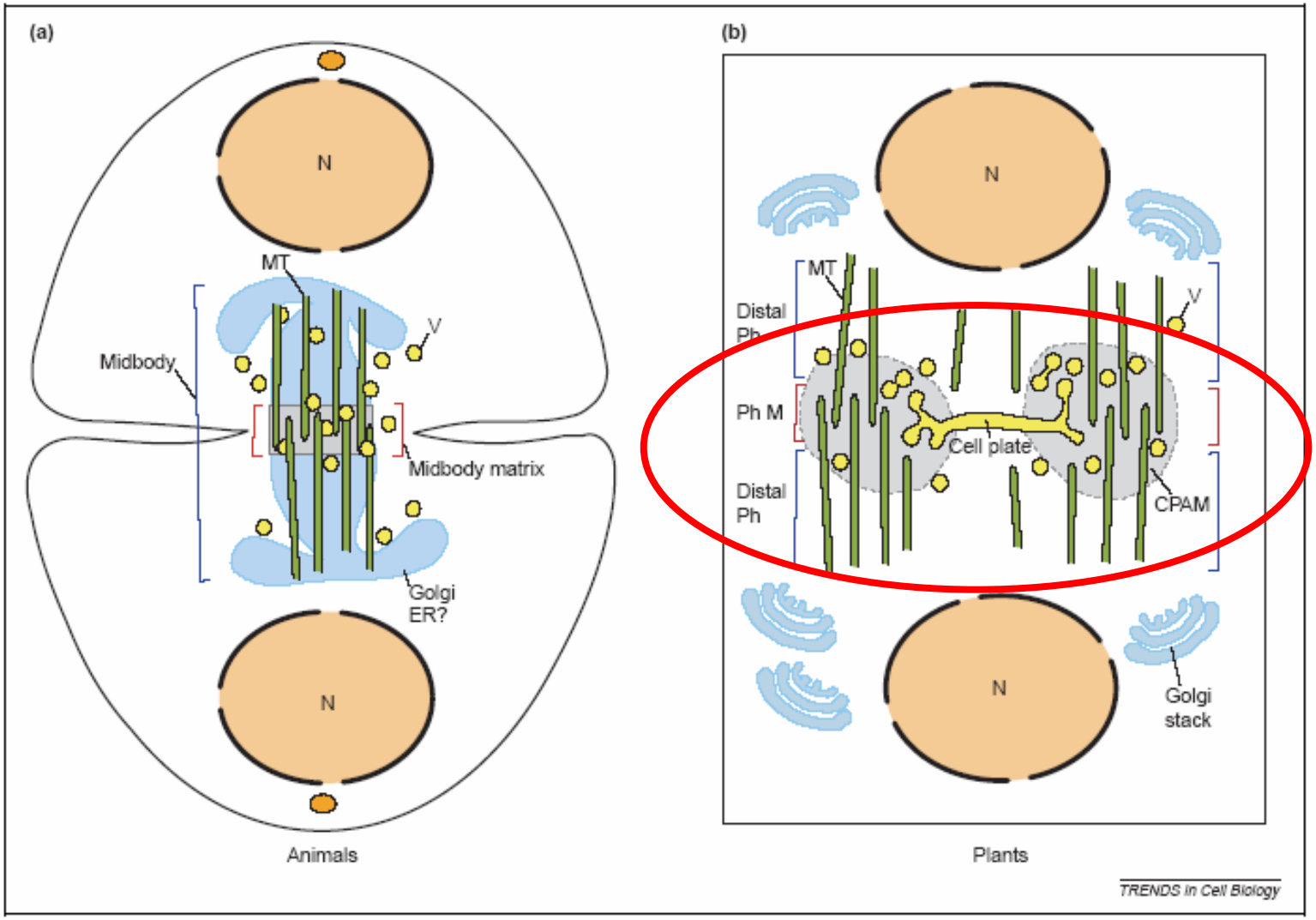

Figure 1. Overview of animal and plant cytokinesis. (a) Cytokinesis in animal cells. The spindle midzone/midbody forms when microtubules (MTs) from opposite poles overlap. It consists of the overlapping microtubules as well as associated proteins that bundle these MTs and other proteins that together form a dense protein matrix. This matrix excludes antibodies against MTs, giving a stereotypical region devoid of staining. As the furrow ingresses, the midzone is swept into one larger structure called the midbody. The Golgi and endoplasmic reticulum (ER) membranes are also found in the midbody during telophase to cytokinesis. It is proposed that vesicles (V) traffic along the midbody microtubules toward the ingressing furrow. (b) Cytokinesis in somatic plant cells. The forming cell plate is assisted by the phragmoplast at the future site of the new cell wall. Two topographic regions can be distinguished in the phragmoplast: the phragmoplast midline (Ph M), where the opposing set of microtubules interdigitate, and the distal phragmoplast (distal Ph), at both sides of the phragmoplast midline. A filamentous cell-plate assembly matrix (CPAM) accumulates at the phragmoplast midline. Key: MT, microtubule (green); N, nucleus (tan); V, vesicle (yellow); Golgi (pale blue); midbody matrix (gray box); CPAM (gray circles).

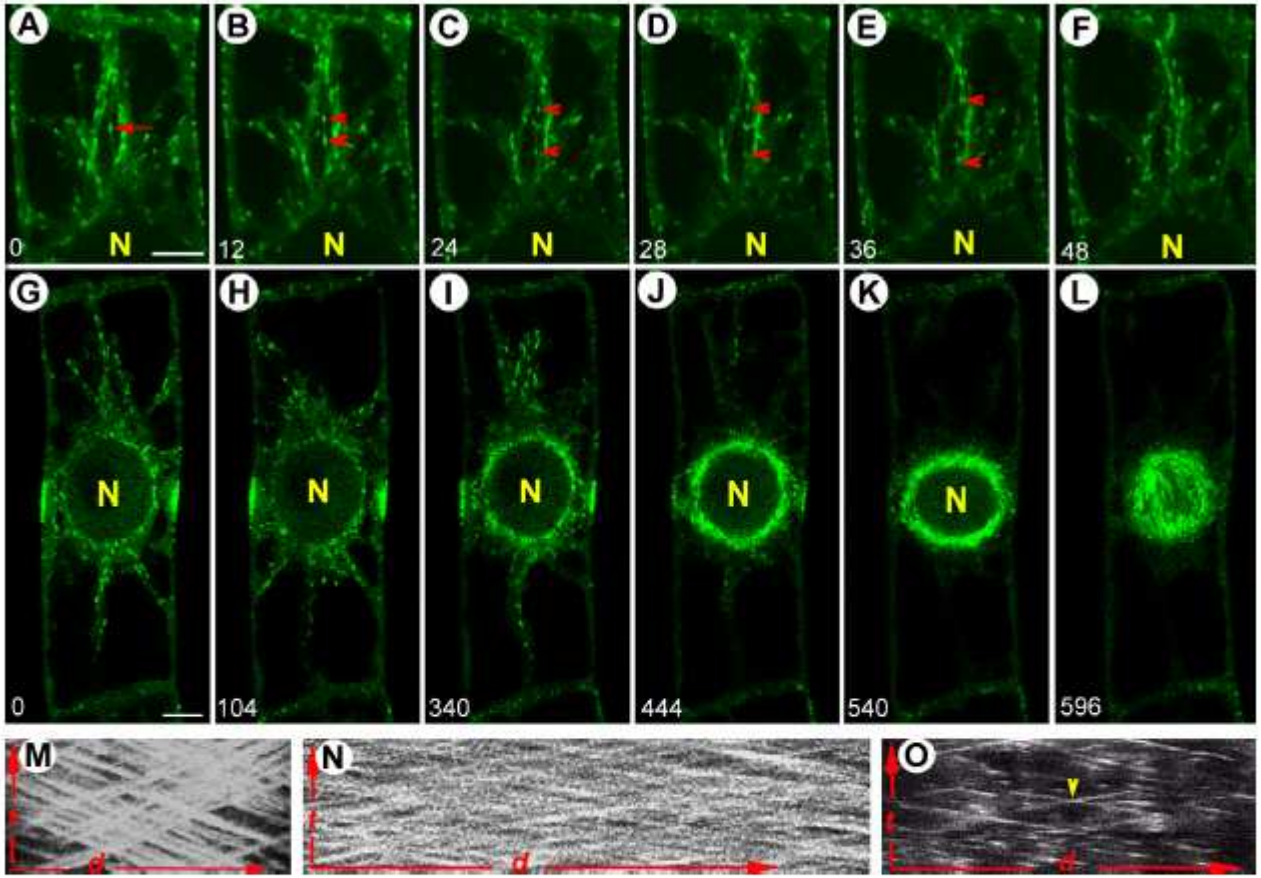

Figure 2
Polarity and growth speed of EMTs bridging nucleus and cortex. Green: GFP-AtEB1 (in A-L). (A-F) EMTs exhibit bidirectional growth and microtubule bundling. Note that that the microtubule originating from the nuclear surface (outgoing) and the one coming from the cortex (incoming) cross each other (arrow) and, as in the cortical array, grow with similar speeds without interfering each other (arrowheads) (see additional file 4: Movie 4). (G-L) EMT plus ends radiating mainly in an outward direction from the NE during PPB maturation (see additional file 5: Movie 5). Kymograph projection of microtubule plus ends in the interphase cortex (M), PPB cortex (N) and preprophase cytoplasm (O) showing sustained polymerization. The horizontal axis, *d*, represents distance (18 μm in M, 13 μm in N and 20 μm in O), and the vertical axis, t, represents time (290 s in M, 140 s in N and 390 s in O). Note that for each of the 3 cases (M-O), the microtubules follow the tracks, exhibit bi-directionality and grow with the same speeds. By comparing the slopes between images M-O, it becomes evident that the microtubule growth speed increases from interphase to the PPB stage, as previously reported [9]. Note that the arrowhead in M shows the crossing of two EMTs growing on the same path at the same time but in opposite directions. Nucleus is marked by 'N', time is indicated in seconds and bars represent 8 μm.

Endocytóza během cytokineze

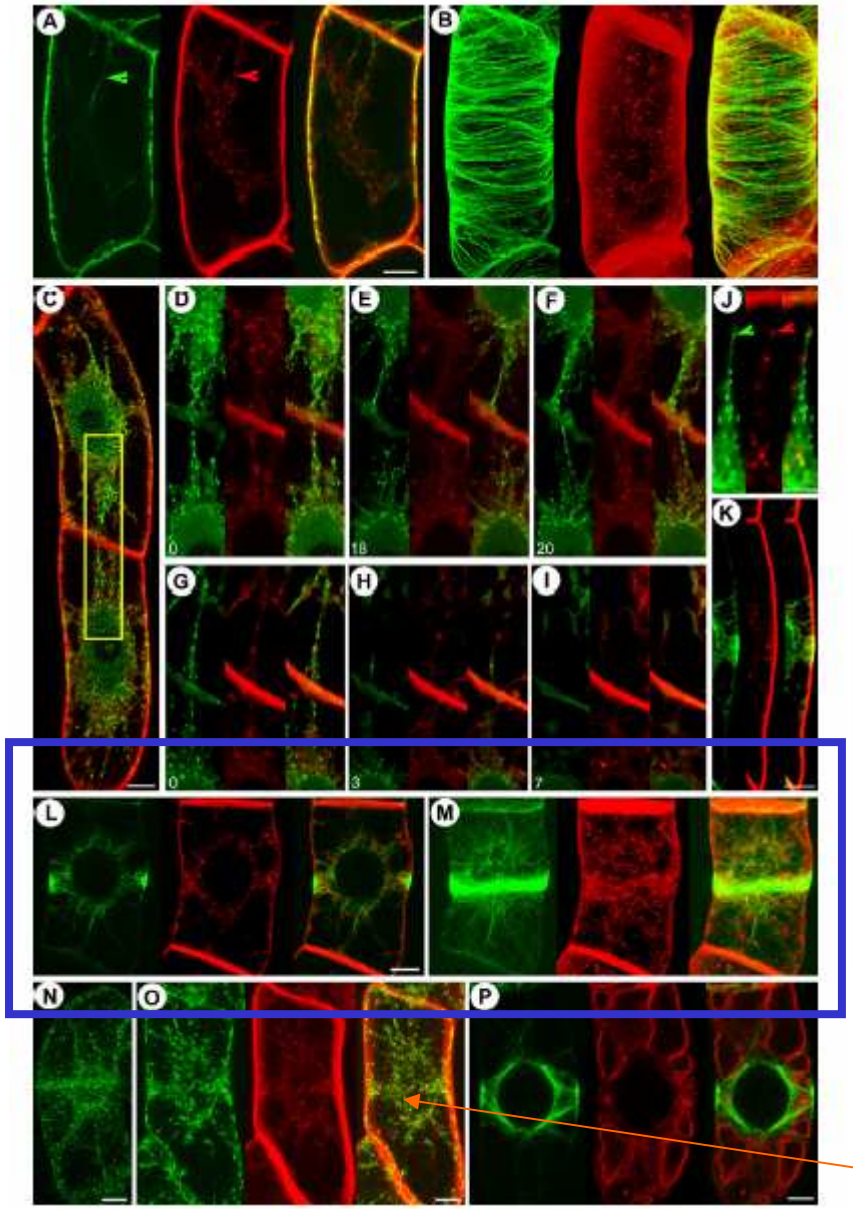

Před nástupem mitózy se tvoří v místě zaostřujícího se preprofázního pásu (PPB) pás zvýšené endocytózy.

Endosomal belt co-localizes with microtubular PPB during preprophase. Green: GFP-MAP4 (in A, B, L, M and P), GFP-AtEB1 (in C-K), GFP-Ara7 (in N) and ST-YFP (in O). Red: FM4-64 (in A-M and O-P). Early in the G2-M transition, FM4-64 labeled endocytic vesicles follow the emerging EMTs labeled with GFP-MAP4, as shown in single median section (A) and 3D-projection (B). The marked rectangle in (C) is zoomed in for (D-I). FM4-64 labeled endocytic vesicles preferentially internalize from the cortical areas approached by the GFP-AtEB1 labeled EMT plus ends (D-F) (see additional file 6: Movie 6), and oryzalin-induced microtubule depolymerization disrupts their internalization routes (G-I) (see additional file 7: Movie 7) whereas the internalization paths are recovered after oryzalin removal (J). (K) Close-up of GFP-AtEB1 marked EMT plus ends bridging the NE and PPB. Note that during PPB narrowing, FM4-64 labeled endocytic vesicles preferentially internalize from the cortical areas approached by the GFP-AtEB1 (see additional file 8: Movie 8). Formation of an FM4-64 labeled cortical belt at the PPB site (labeled with GFP-MAP4) is shown in a single median section (L) and in 3-D projection (M). (N) 3-D projection of GFP-Ara7 labeled endosomes exhibiting an endosomal belt at preprophase. (O) Both FM4-64 labeled endosomes and ST-YFP labeled GAs form a cortical belt at the PPB site. (P) GFP-MAP4 labeled EMTs connecting the nucleus to the PPB intersect FM4-64 labeled vacuoles. Time is indicated in minutes. Bars represent 7 μm in A, B, J, L, M, 10 μm in C, N-P and 5 μm in K.

GFP-MAP4 = marker mikrotubulů

GFP-EB1 = marker (+)-konců mikrotubulů

Golgi + endosomy

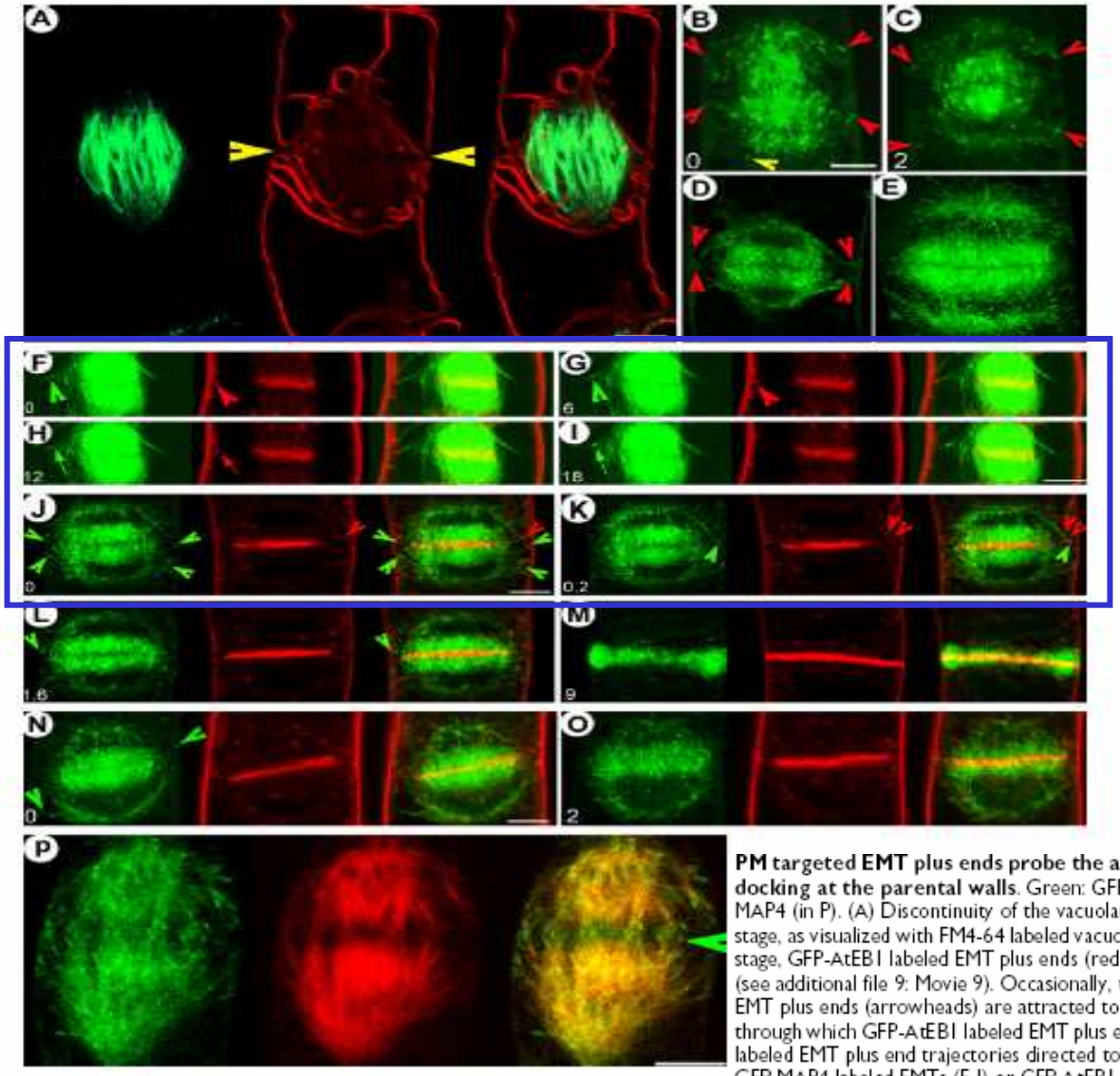

F–K: EMTs (Endoplasmic MTs) dorůstají do oblasti předchozího PPB a tak se setkávají s endosomy, které po nich putují v minus-směru.

PM targeted EMT plus ends probe the areas occupied by the preceding PPB and align the cell plates for proper docking at the parental walls. Green: GFP-MAP4 (in A, F-I), GFP-AtEB1 (in B-E, J-O and P). Red: FM4-64 (in A, F-O), YFP-MAP4 (in P). (A) Discontinuity of the vacuolar structures in the preceding PPB site (arrowheads) is maintained at the spindle stage, as visualized with FM4-64 labeled vacuoles and GFP-MAP4 labeled microtubules.(B-C) At the onset of the phragmoplast stage, GFP-AtEB1 labeled EMT plus ends (red arrowheads) originating from the former spindle poles grow towards the cortex (see additional file 9: Movie 9). Occasionally, they grow towards the polar areas (yellow arrowhead). (D) GFP-AtEB1 labeled EMT plus ends (arrowheads) are attracted to the cortical areas marked by the preceding PPB. At late telophase, the distance through which GFP-AtEB1 labeled EMT plus ends reach towards the cortex is reduced. (E) 3-D projection showing GFP-AtEB1 labeled EMT plus end trajectories directed towards the cortex, which are different from the main phragmoplast structure. GFP-MAP4 labeled EMTs (F-I) or GFP-AtEB1 labeled EMT plus ends (J-M) continue to reach the cortex at the former PPB site and display close proximity to FM4-64 labeled endosomes (red arrow and arrowheads). These endosomes display movement towards the minus end of these EMTs. (N-O) GFP-AtEB1 labeled plus end growth of EMTs (arrowheads) towards opposite sides of the cortex is maintained during cell plate and phragmoplast tilting (see additional file 10: Movie 10). (P) Enrichment of GFP-AtEB1 labeled microtubule plus ends (arrowhead) but not of YFP-MAP4 labeled microtubular parts at the phragmoplast midline. Time in F-I is given in seconds while that in J-O is indicated in minutes. Bars in A-O represent 8 μm while that in P represents 10 μm.

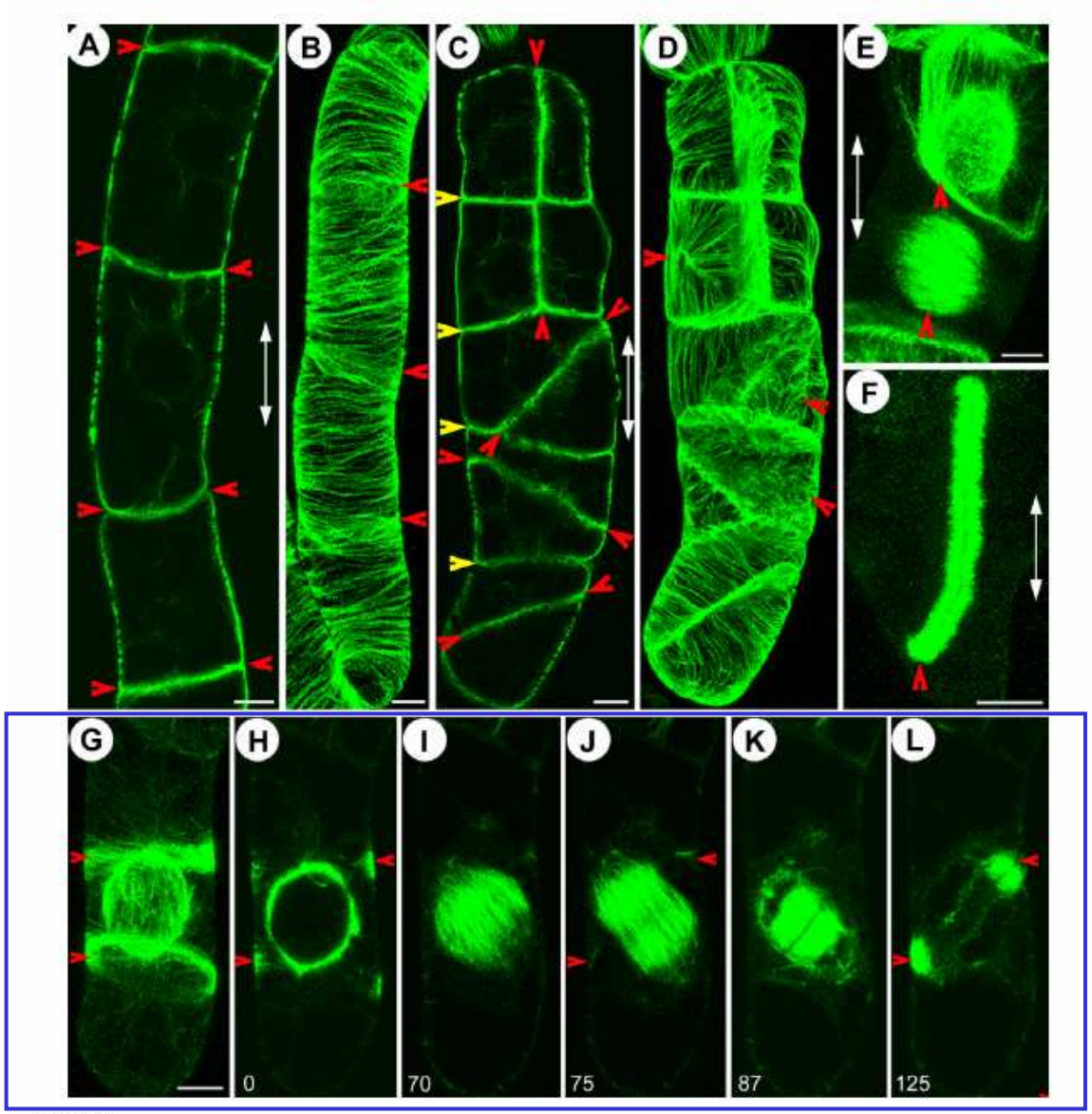

Figure 6
NPA induces abnormal PPBs and altered cell divisions. (A-B) Normal anticlinal cell divisions (arrowheads in A) and transverse organization of cortical microtubules in NPA untreated cells. (C-D) Inclined and periclinal cell divisions (red arrowheads in C) with altered organization of GFP-MAP4 labeled cortical microtubules (red arrowheads in D) in NPA treated cells. A, C show single median sections and B, D show 3-D projections. Note that the first round of cell division (yellow arrowheads) is normal and a shift in the cell division planes occurs in the second round. (E-F) Formation of periclinal PPBs and spindles (arrowheads in E) and periclinal phragmoplasts (arrowhead in F). Bidirectional arrows in A, C, E and F show the long axes of the cells. (G-L) NPA treatment sometimes causes formation of two separate PPBs (arrowheads in G) equidistant from the nucleus, which results in tilted spindle formation (I) and phragmoplast initiation (J), phragmoplast growth (K) and cell plate docking (L) at sites marked by either of the PPBs (arrowheads) (see additional file 11: Movie 11). G shows 3-D projection and H-L show single median sections. Bars represent 10 μm and time is indicated in minutes.

Inhibitor transportu auxinu NPA (naphthylphtha-lamic acid) narušuje tvorbu PPB a orientaci buněčné přepážky.

Endocytóza během cytokineze

- Endocytóza je intenzivní v místech kde se endoplasmatické MTs setkávají s PPB.
- Pás endosomů proto leží v těsné blízkosti PPB a je zachován i po rozpadu PPB při tvorbě mitotického vřeténka.
- Kyselina naftylftalamová (NPA), inhibitor polárního výtoku auxinu, působí anomální PPBs a následně posuny v rovině buněčného dělení.

Dynamika cytoskeletu
je neoddělitelně a recipročně provázána
s dynamikou endomembránového systému.

Vakuola

či spíše vakuol**y**

MNOHOTVARÝ KOMPARTMENT ROSTLINNÝCH BUNĚK

Ve vakuole dochází k **nespecifické** degradaci řady substrátů včetně lipidů, polysacharidů a bílkovin. Má zásadní význam pro transport iontů – vody a tedy turgor. Má funkci zásobní, signální – a „přežívací“(autofagie).

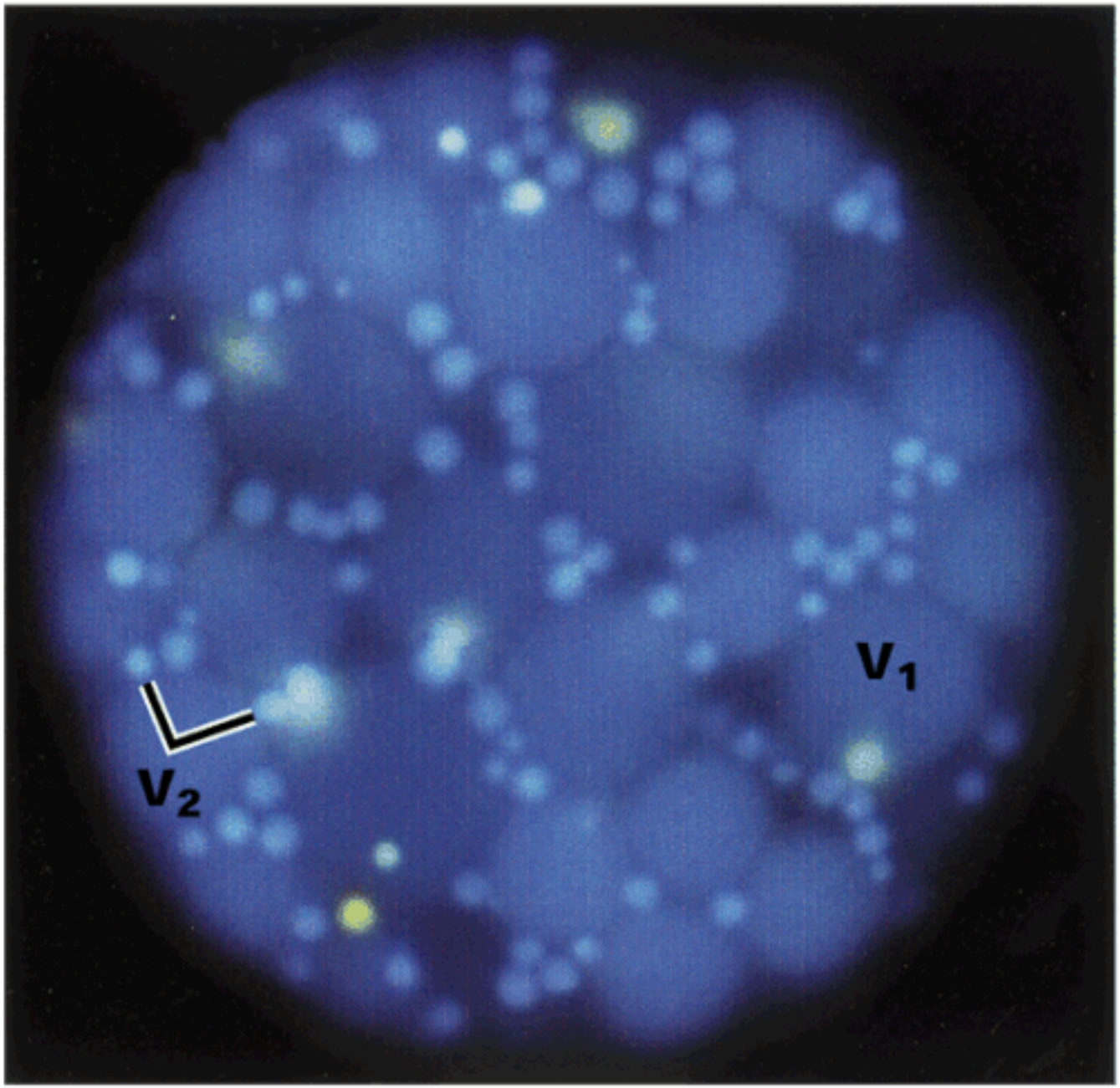

protoplast aleuronu kukuřice

V1
protein storage vacuole (PSV)

V2
lytic vacuole (LV)

Vakuola

Vakuola je topologicky extracytoplasmatický kompartment.

Velmi rychle se vyrovnává se změnami osmotických poměrů v apoplastu.

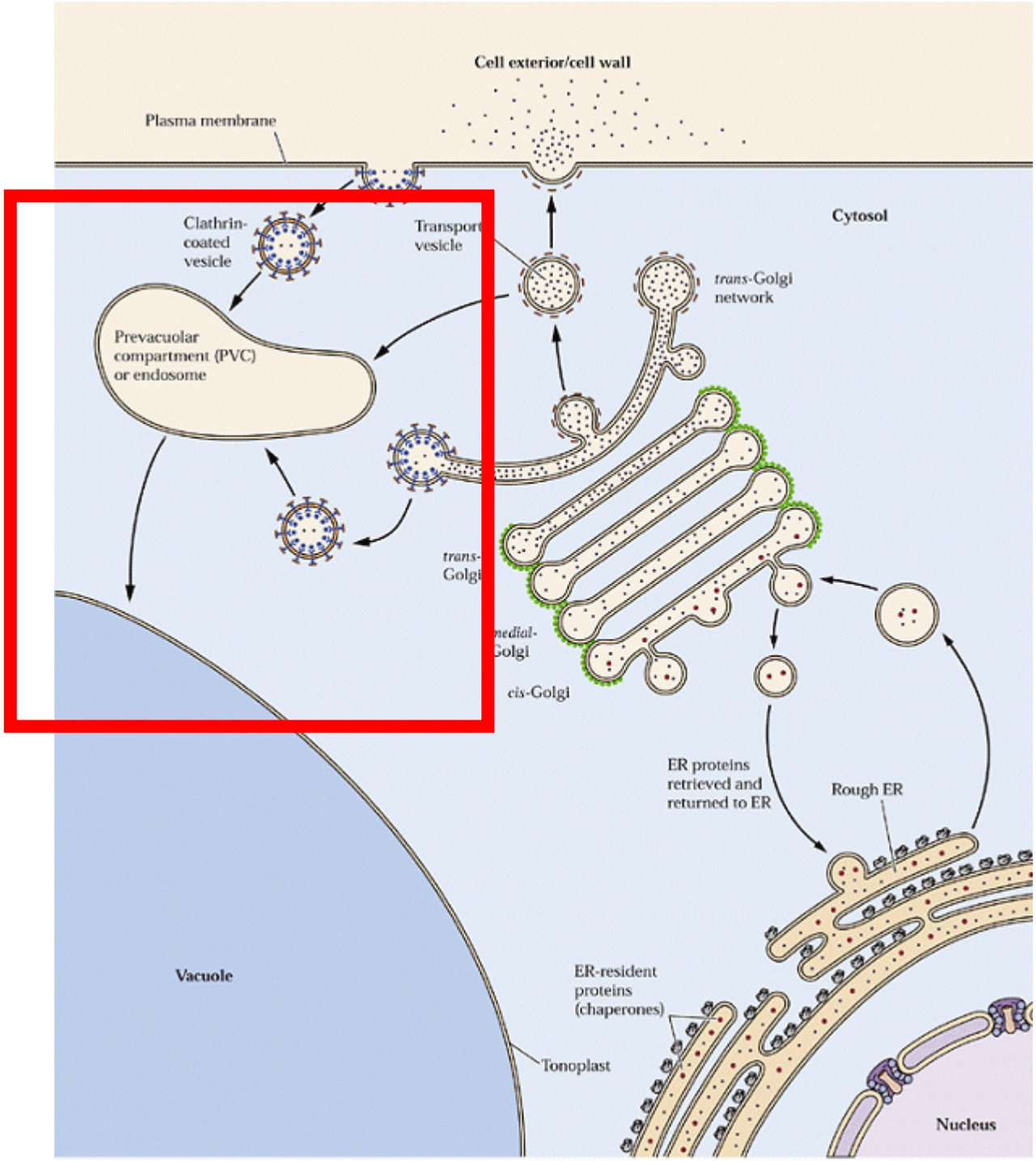

Δ*pep12*

Δ*pep12*+
S.c. PEP12

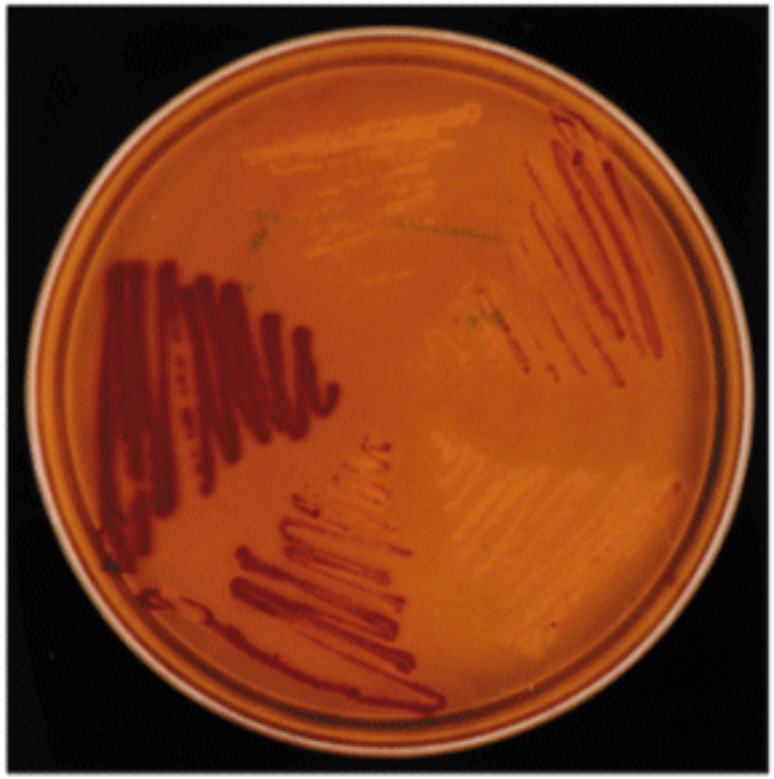

Δ*pep12*+
A.*t.* cDNA2

Δ*pep12*+ unrelated
A.*t.* cDNA

Δ*pep12*+
A.*t.* cDNA1

PEP12 je prevakuolární t-SNARE u Arabidopsis – UŽITÍ JAKO MARKERU

Vakuolární lokalizační signály

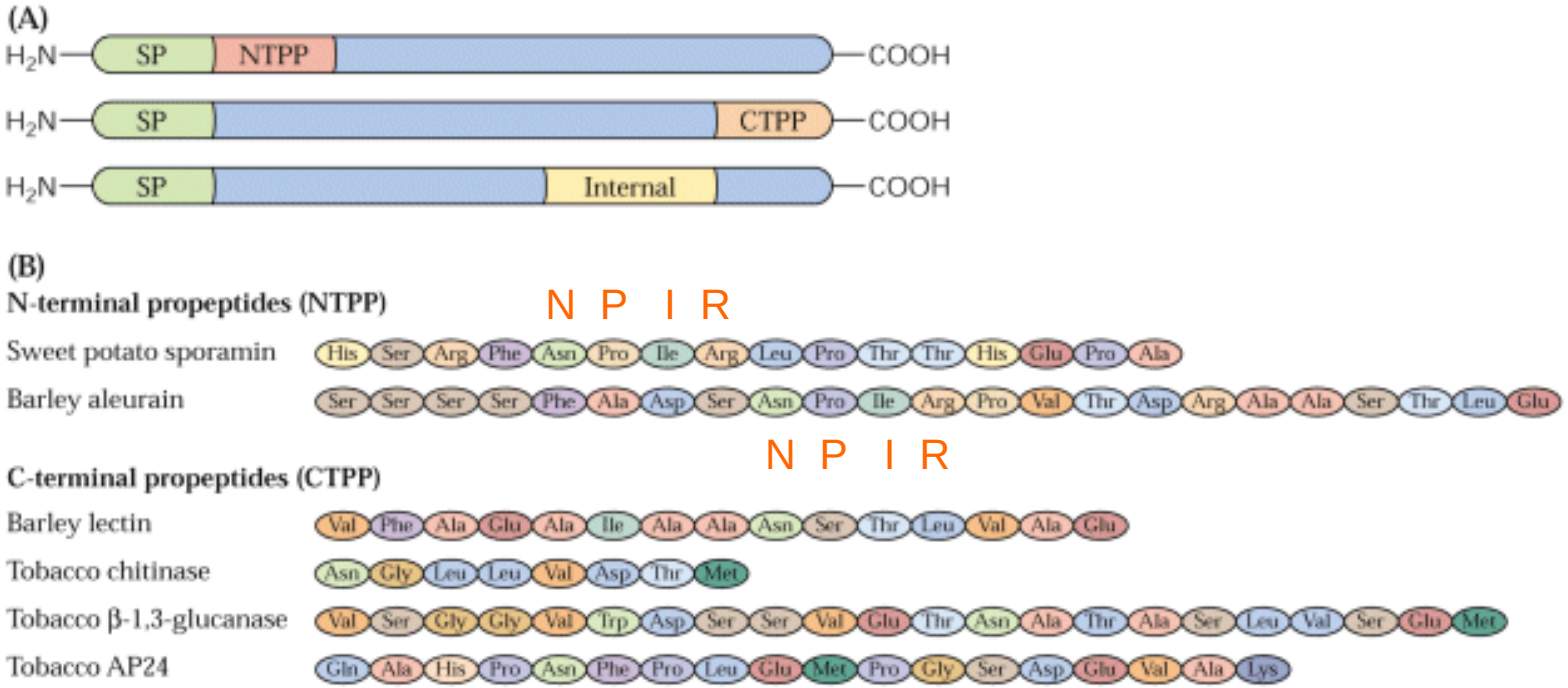

TŘÍDĚNÍ DO VAKUOLY

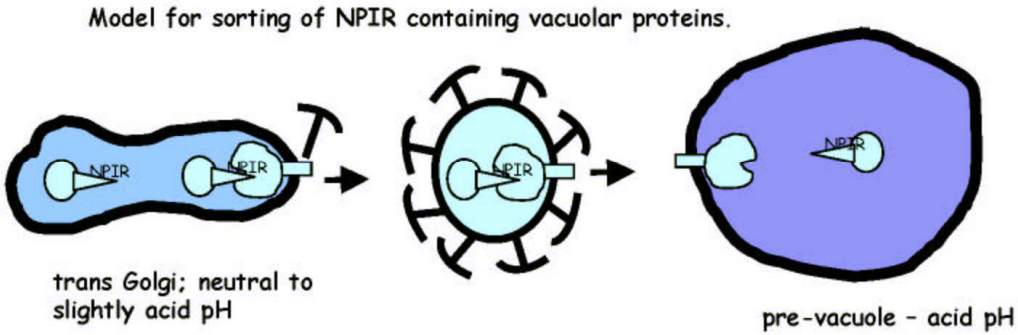

Kirsch T, Paris N, Butler JM, Beevers L, Rogers JC. Purification and initial characterization of a potential plant vacuolar targeting receptor. Proc Natl Acad Sci. 1994. 91:3403-7.

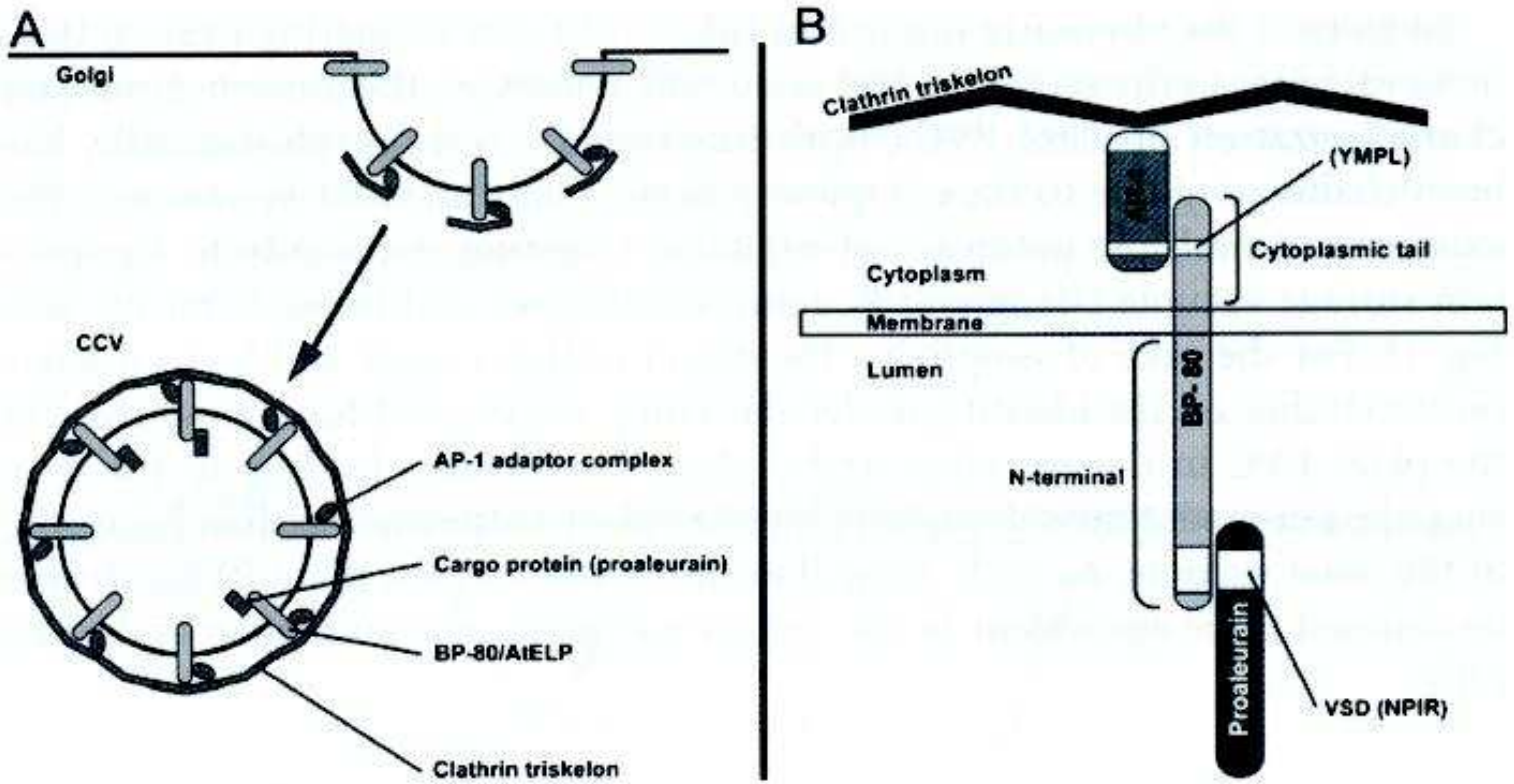

Fig. 2 Working model of receptor-mediated sorting in plants. Depicted are the possible interactions between the receptor BP-80 and the cargo protein proaleurain in the trans-Golgi network (TGN). **A** Formation and budding of clathrin-coated vesicles (CCVs) at the TGN. **B** Specific protein components and their interactions within a CCV. AP-1, adaptor protein complex AP-1; NPIR, vacuolar sorting determinant (VSD) from proaleurain; YMPL, tyrosine motif from the cytoplasmic tail of BP-80

Třídění do lytické vakuoly přes BP-80/ELP receptory.

(A) Transport to PSV in dense vesicles

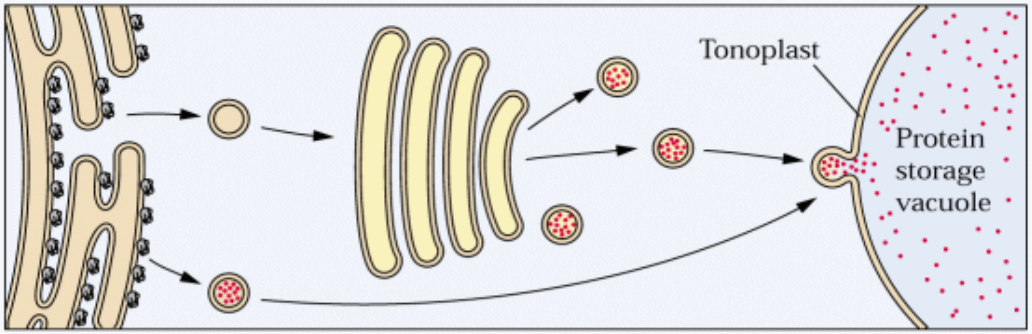

(B) Transport in CCV to lytic vacuoles

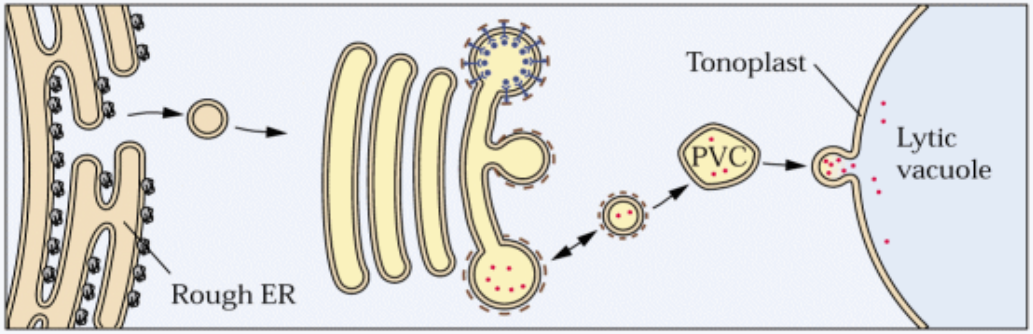

(C) Transport of prolamins by autophagy

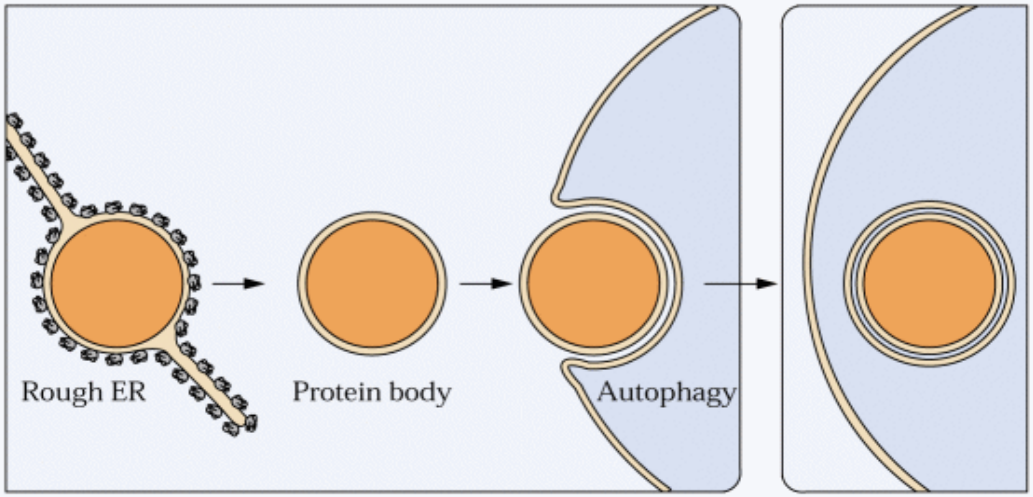

Prolaminy

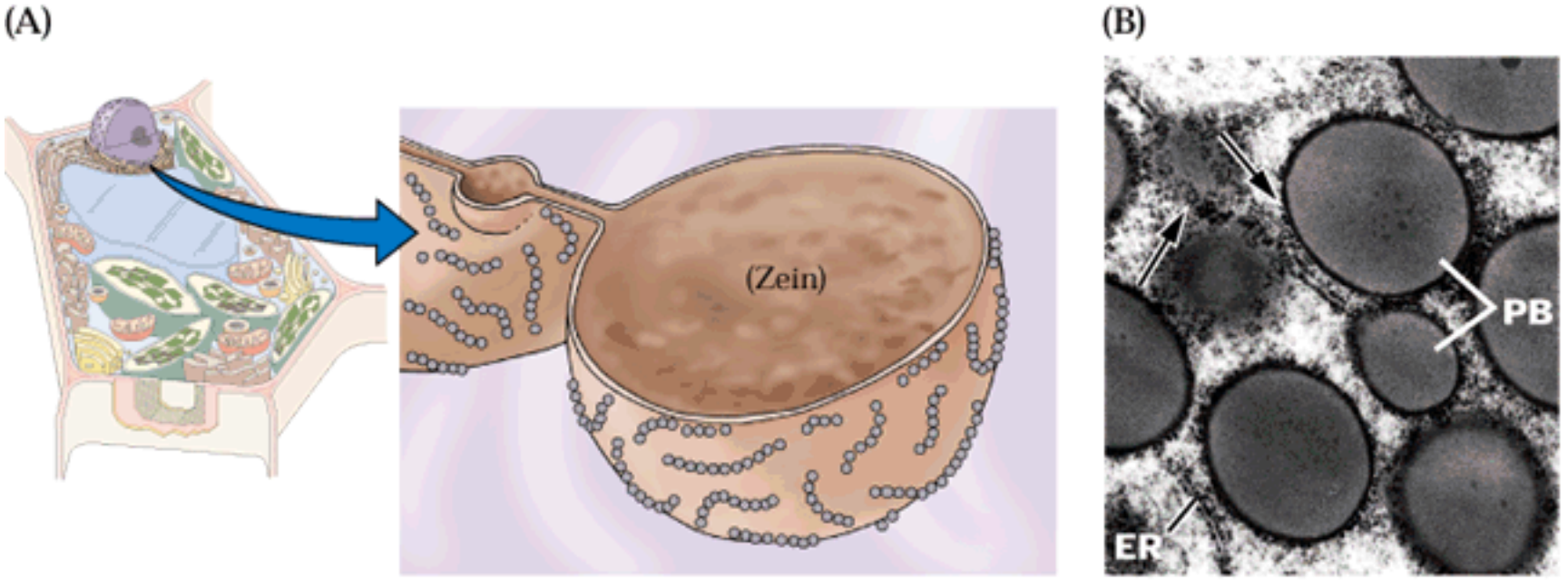

Agregace jako třídící mechanismus v ER - PB.

Lokalizovaná translace na spec. doménách ER.

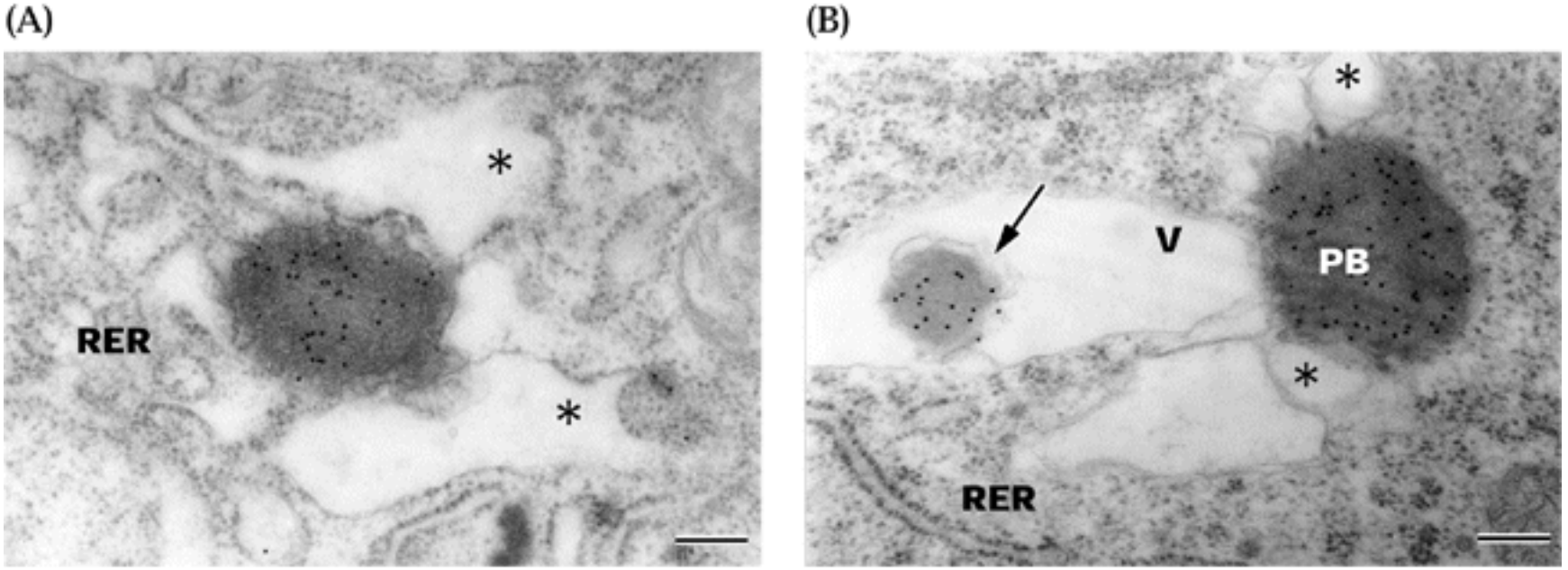

Od ER odvozená PB jsou obklopována a pohlcována vakuolami.

Podstatnou součástí třídění leguminů je jejich postupná agregace v periferních oblastech GA.

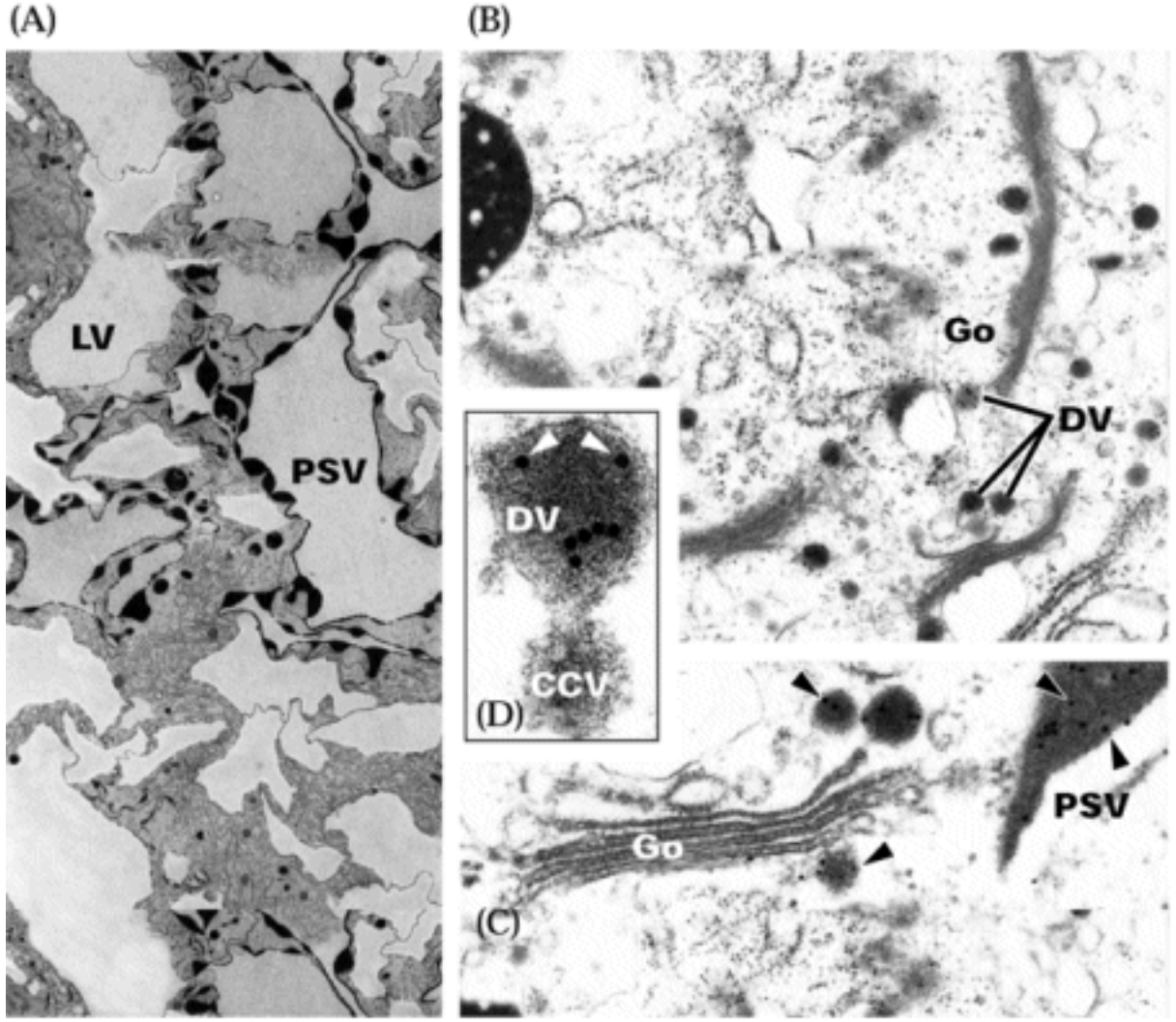

Clathrin coated vesicles, které vznikají na PB doménách GA pravděpodobně odtřiďují složky, které do PSV nepatří.

Tvorba prevakuolárního komp.- MVB – pozdního endozómu

bodies. Eventually, all of the internal membranes produced by the invaginations shown are digested by proteases and lipases in lysosomes. The invagination is essential to achieve complete digestion of endocytosed membrane proteins. Because the outer membrane of the multivesicular body becomes continuous with the lysosomal membrane, lysosomal hydrolases could not digest the cytosolic domains of transmembrane proteins such as the EGF receptor shown here, if it were not for the invagination.

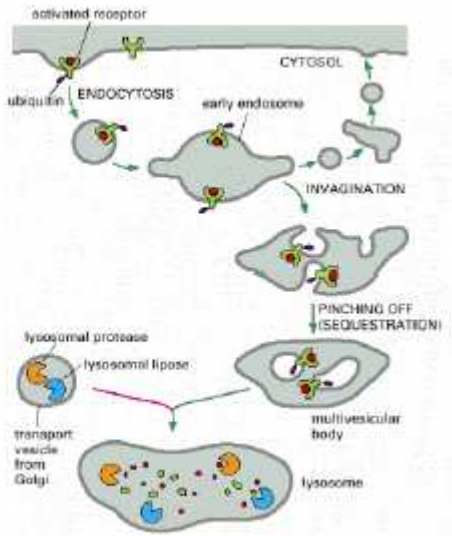

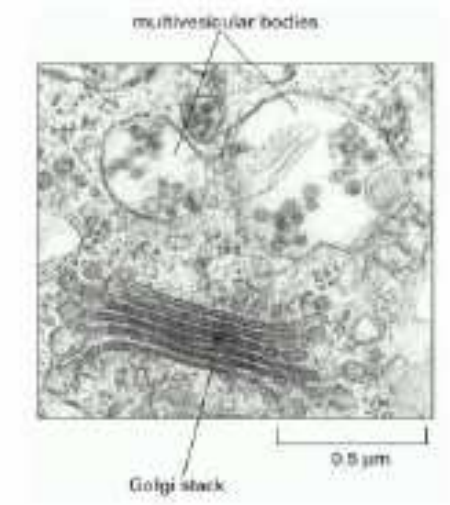

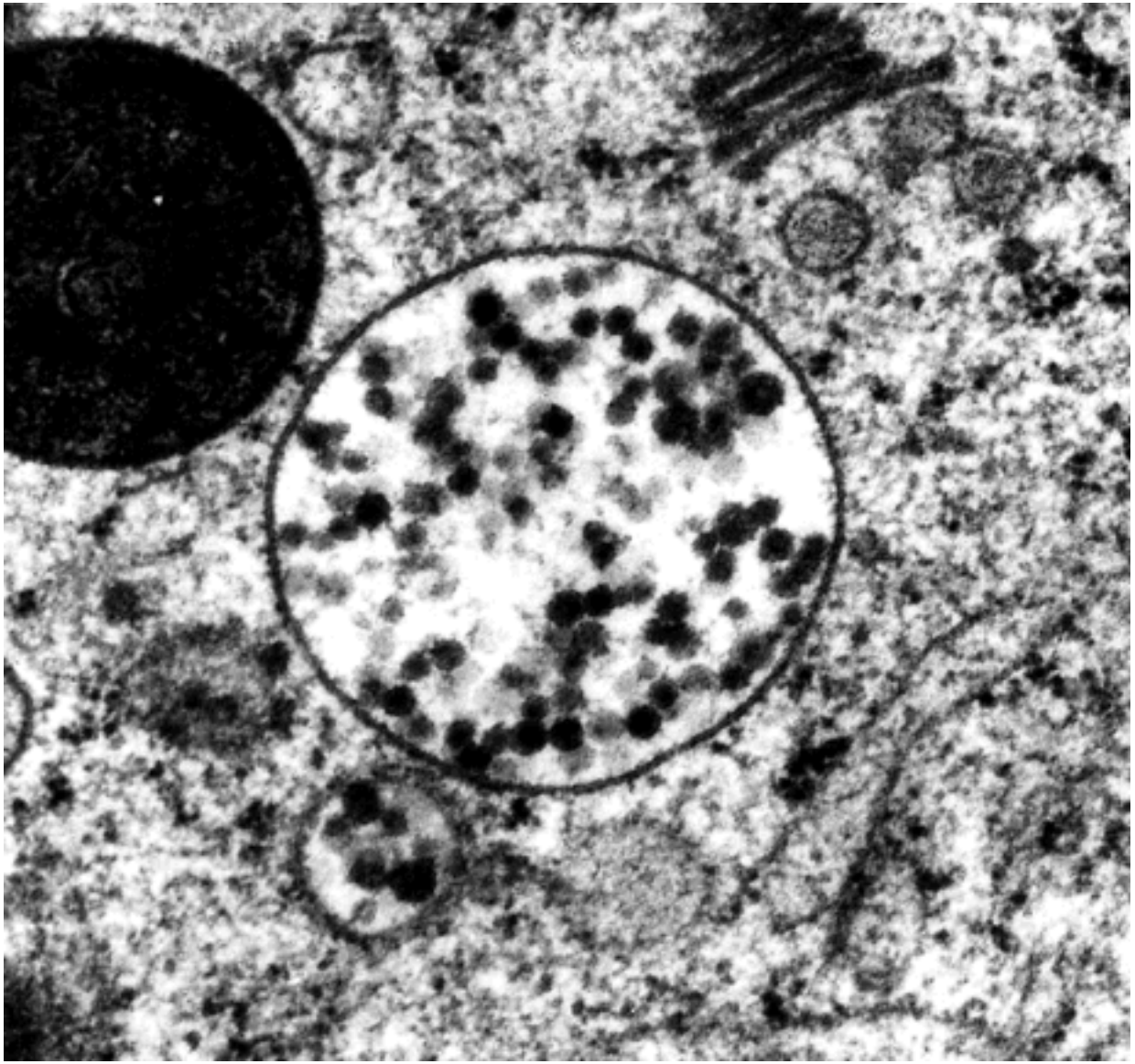

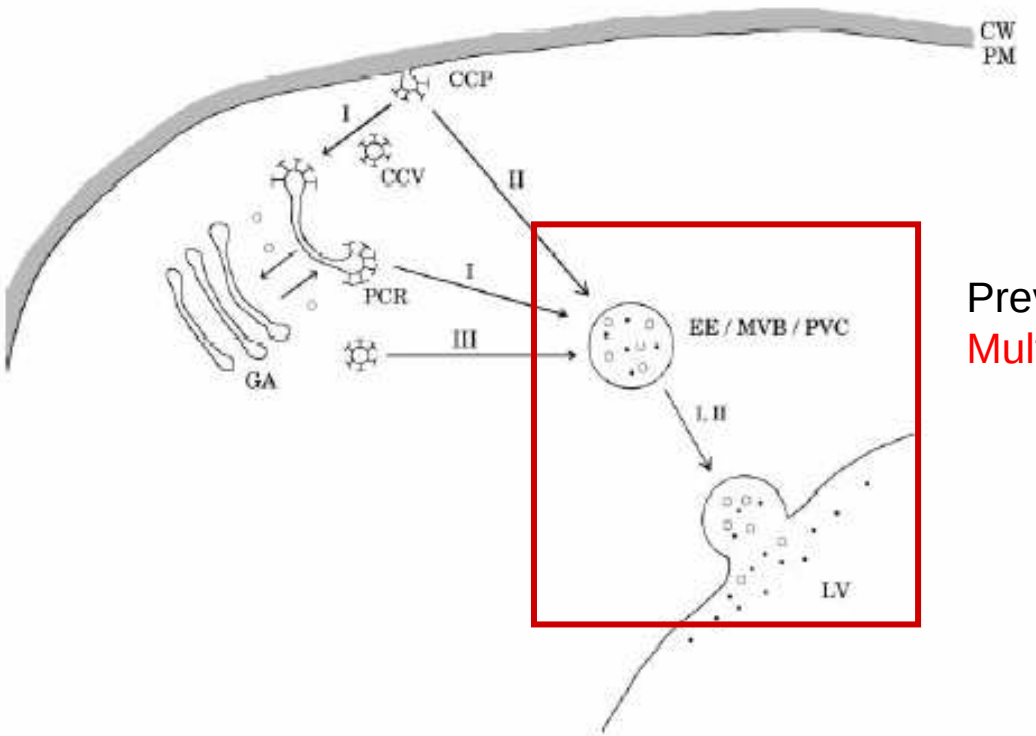

Prevacuolar compartment
Multi Vesicular Body

Figure 1: The endosomal system of a model plant cell. *Route I:* The time-course of the clathrin-dependent internalization of electron-dense markers can be considered established. Thus, after budding from the clathrin-coated pit (CCP) endocytosed markers first appear in the partially coated reticulum (PCR) and in the Golgi region (GA). Along this route the next compartments are the multivesicular bodies (MVB) and finally the lytic vacuole (LV). *Route II:* FM-labeled plasma membrane (PM) is delivered to a Rab5-positive putative early endosomal compartment (EE), but the dependency on clathrin for the uptake at the PM remains to be shown. *Route III:* Soluble proteins bound to the vacuolar sorting receptor (AtELP) destined for the lytic vacuole are delivered via CCV from the Golgi to a prevacuolar compartment (PVC). Several classes of proteins involved in intracellular transport have been described for the following locations: *PM:* Phragmoplastin, SYP111, SYP121, SNAP33, Ara6; *EE:* Ara6, Ara7; *PVC:* AtELP, SYP21, SYP22, SYP51, VTI11. *CW:* cell wall. See text for more details..

Třídění bílkovin z MVB **do** vakuoly je řízeno třemi (I,II,III) komplexy **ESCRT** - u Arabidopsis jsou některé podjednotky známy díky analýze mutantů ***hyade***.

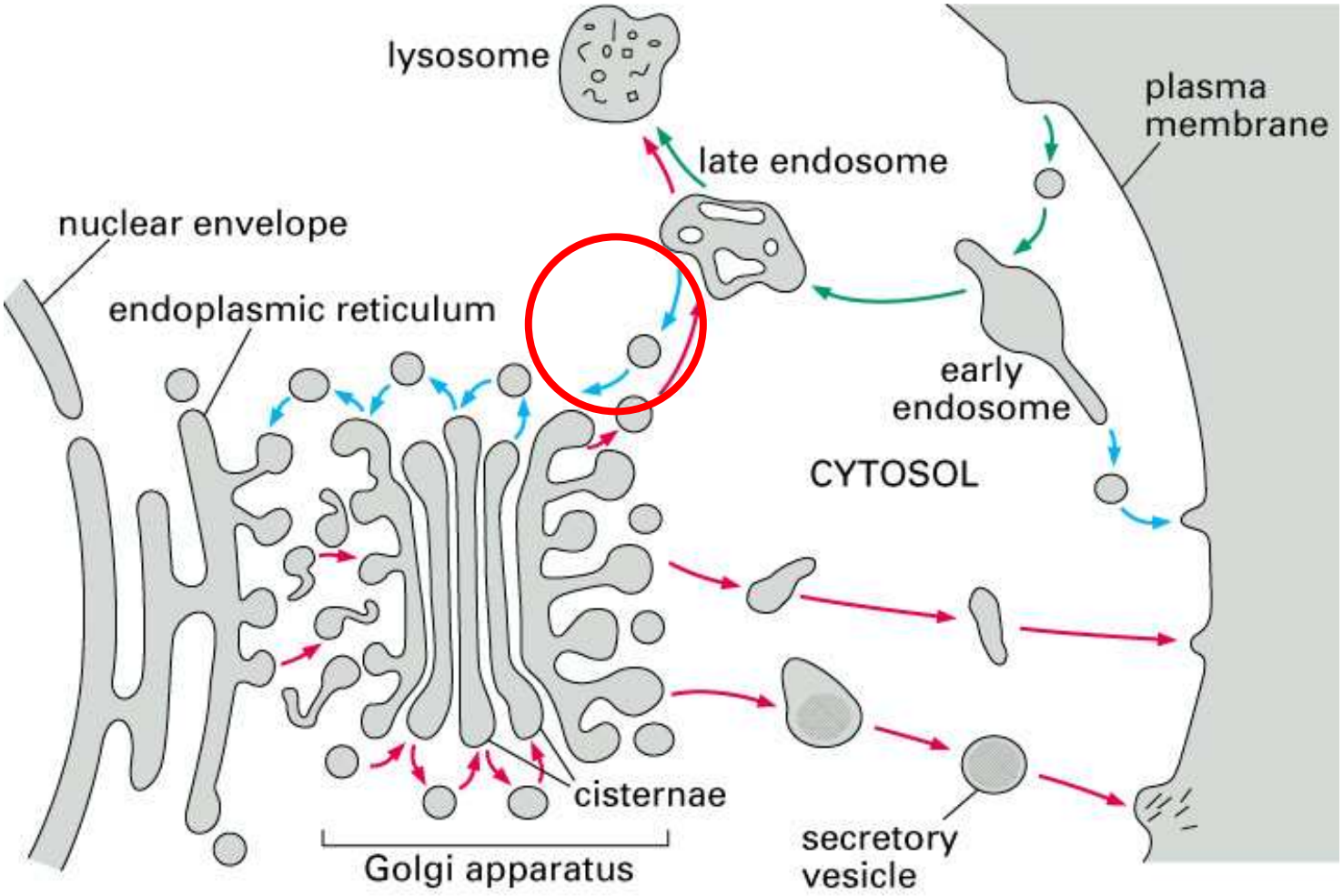

Figure 13–3. Molecular Biology of the Cell, 4th Edition.

Komplex **Retromer** pomáhá **recyklovat** z PVC do TGN

Vesicular traffic and the role of Golgi apparatus (body) as a “traffic controller”. Protein modifications take place in the Golgi, which result in acquisition of appropriate signals, and hence packaging into correct vesicles. Hydrolytic enzymes are sent to lysosome, export vesicles to plasmalemma and ER membranes and proteins are recycled back to ER (**Fig 13-21**).

Komplex **RETROMER**

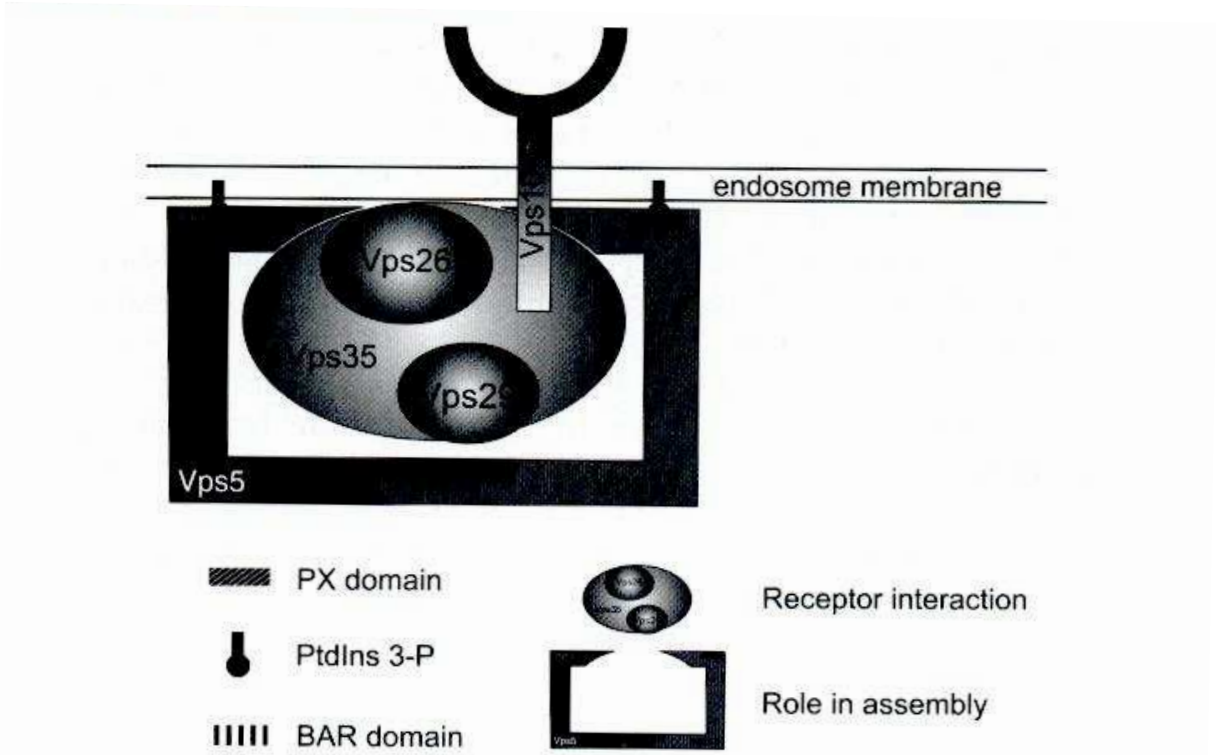

Fig. 5 The molecular components of the retromer complex. Shown are the relationships between the yeast vacuolar sorting receptor Vps10p and the components of the two retromer subunits

Homology jsou také u rostlin a je pravděpodobné, že funguje podobně.

Rostliny jsou schopny přežívat fáze nedostatku živin mj. také díky bohatě rozvinuté schopnosti autofagie - degradace cytoplasmatických částí ve speciální vakuole.

Autofagická vakuola

4 dráhy

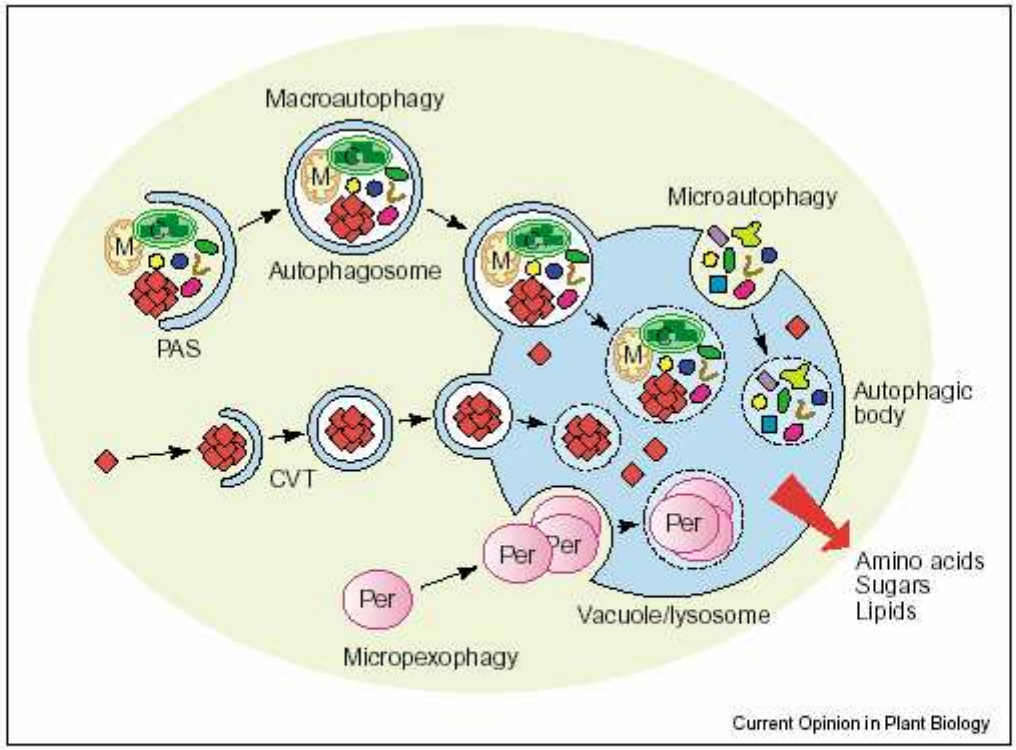

Morphological steps during microautophagy, macroautophagy, CVT, and micropexophagy. Micropexophagy and microautophagy proceed by invagination of the tonoplast to engulf portions of the cytosol and peroxisomes (Per) to create autophagic bodies within the vacuole. Conversely, both macroautophagy and CVT sequester cytosolic components in a double membrane-bound vesicle, which then fuses with the tonoplast to release its contents into the vacuolar lumen. For macroautophagy, this vesicle is called the autophagosome. Where appropriate, the cargo is degraded by resident vacuolar hydrolases; the products are either stored in the vacuole or transported back to the cytosol for reuse. Adapted from [33]. C, chloroplast. M, mitochondrion.

CVT = cytoplasm to vacuole targeting

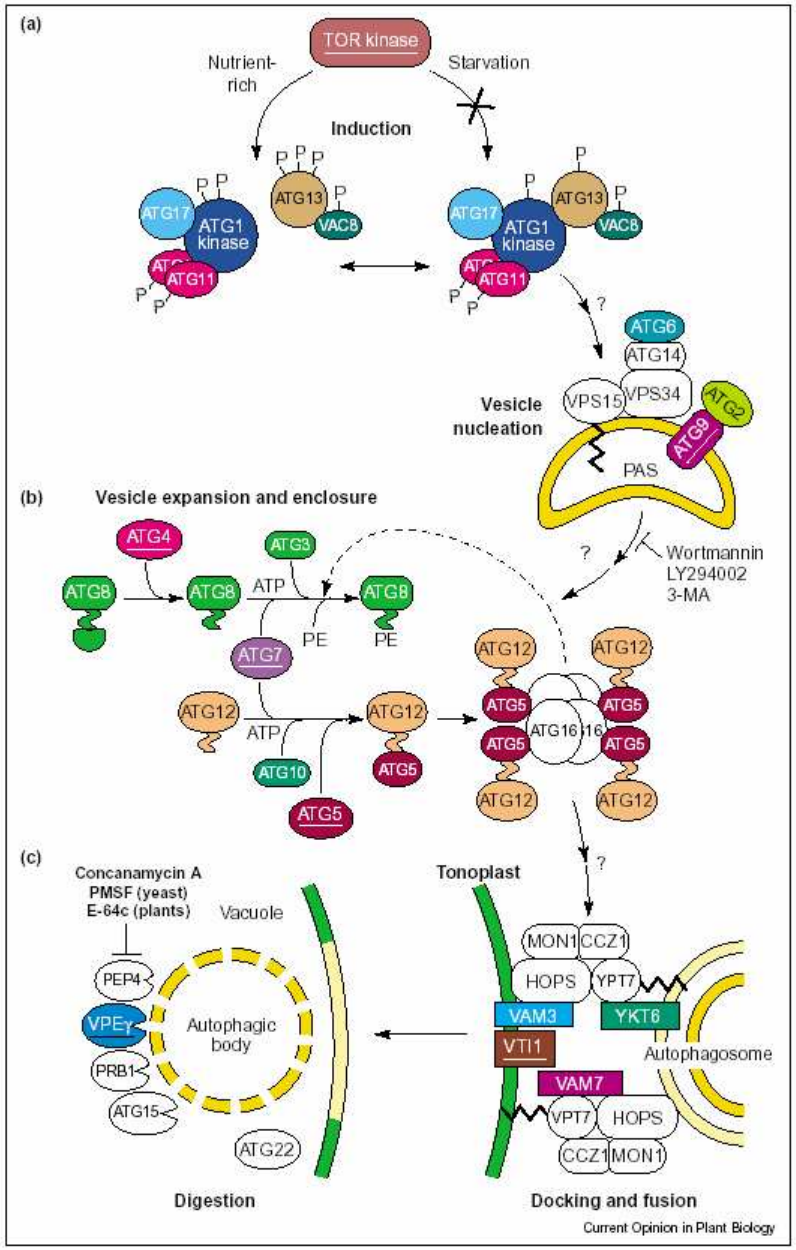

Schematic representation of known components within the ATG autophagic pathways in yeast and *Arabidopsis*. **(a)** Induction of the ATG pathway is regulated by the nutritional status of the cell. Under nutrient-rich conditions, the TOR kinase hyperphosphorylates the ATG1 kinase and ATG13, promoting their dissociation from a complex that contains the accessory factors ATG11, ATG17, and VAC8. Under nutrient-poor conditions, ATG1 and ATG13 are dephosphorylated, which in turn promotes the re-association and activation of the kinase complex. The active ATG1–ATG13 kinase complex promotes nucleation of the PAS to form the autophagosome in a process involving the PI3K VPS34, the transmembrane protein ATG9, and other factors. This step is blocked by the PI3K kinase inhibitors wortmannin, LY294002 and 3-MA. **(b)** Engulfment by the PAS is achieved with the help of two ATP-dependent Ub-like conjugation systems that involve the tags ATG8 and ATG12,

Bílkoviny řídící tvorbu autofagických vakuol jsou dobře evolučně konzervovány.
Celá dráha je aktivována TOR kinázou a pak procesem podobným ubiquitinaci.
Důležitou roli hraje PI3K - VPS34, která je inhibována wortmanninem.

5 month SD

Bez dusíku

Ve tmě

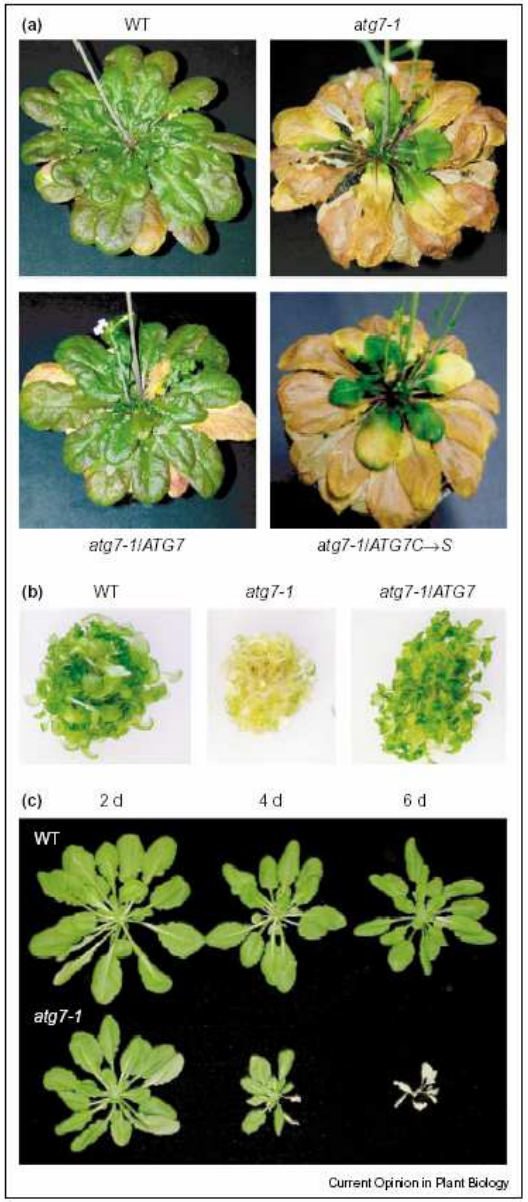

Phenotypes of an *Arabidopsis* mutant that is affected in the *ATG7* gene, which encodes the E1 required for activation of ATG8 and ATG12 before their conjugation to PE and ATG5, respectively. Plant lines include wildtype *Arabidopsis* (WS ecotype), the *atg7-1* mutant, and the *atg7-1* mutant complemented with either *ATG7* or a mutation in which the active-site cysteine codon was converted to that for a serine (*ATG7C→S*). **(a)** Early senescence of rosette leaves. Five-month-old plants grown in nutrient-rich soil under a short-day photoperiod (from [25]). **(b)** Plants grown for 32 days in nitrogen-free liquid medium. **(c)** Plants exposed to dark-induced carbon starvation. Six-week-old plants were grown under an 8 hour light/16 hour dark short-day photoperiod, transferred to darkness for 2, 4 or 6 days and then transferred back to the short-day period for one week (AR Thompson *et al.*, unpublished).

Arabidopsis s postiženou tvorbou autofágních vakuol rychleji stárne a hůře odolává hladovění.

Vakuoly jsou centrální pro život rostlinné buňky

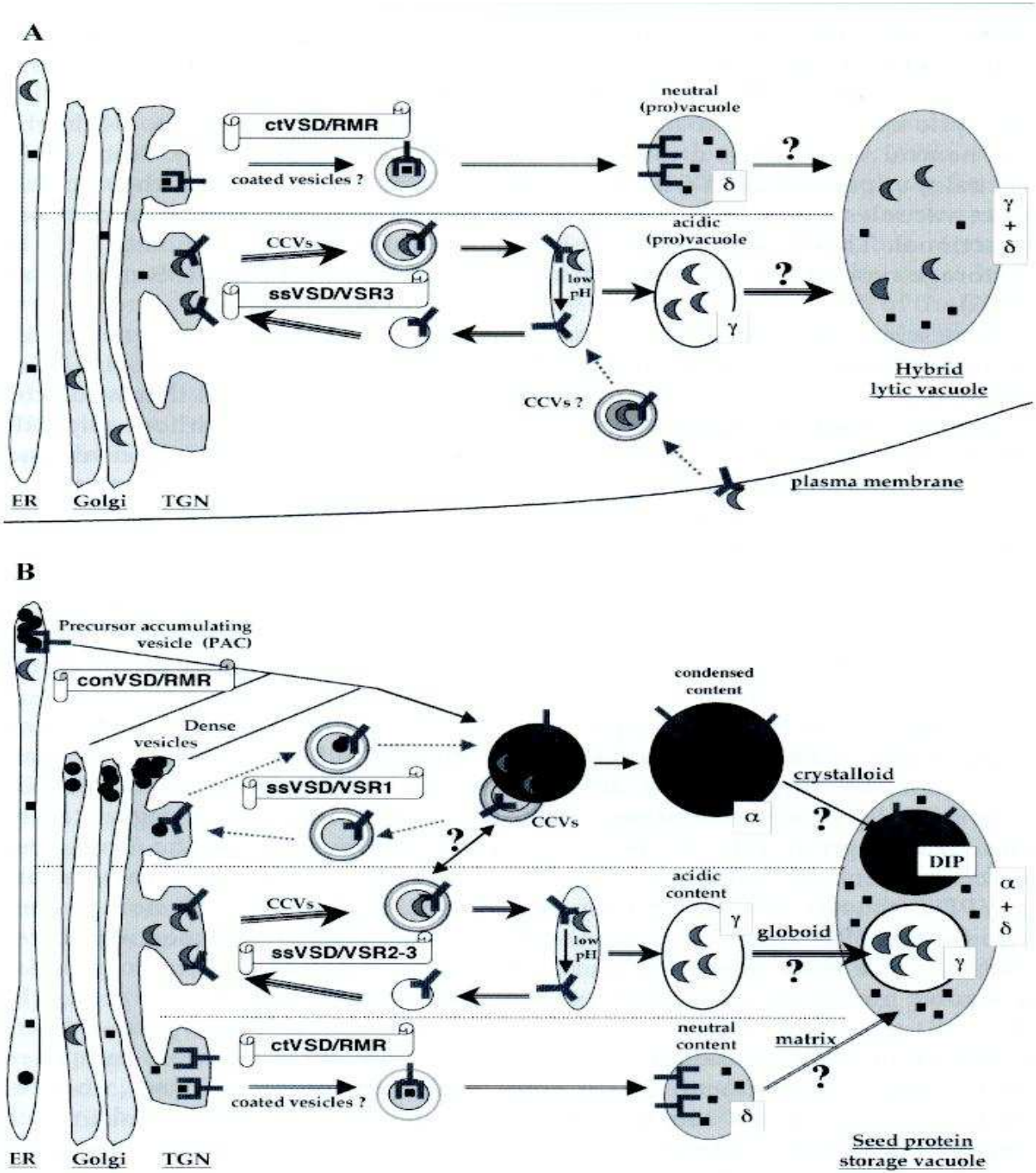

Robinsonovy shrnující modely (2005)

KANÁLY, PŘENAŠEČE A PUMPY TONOPLASTU

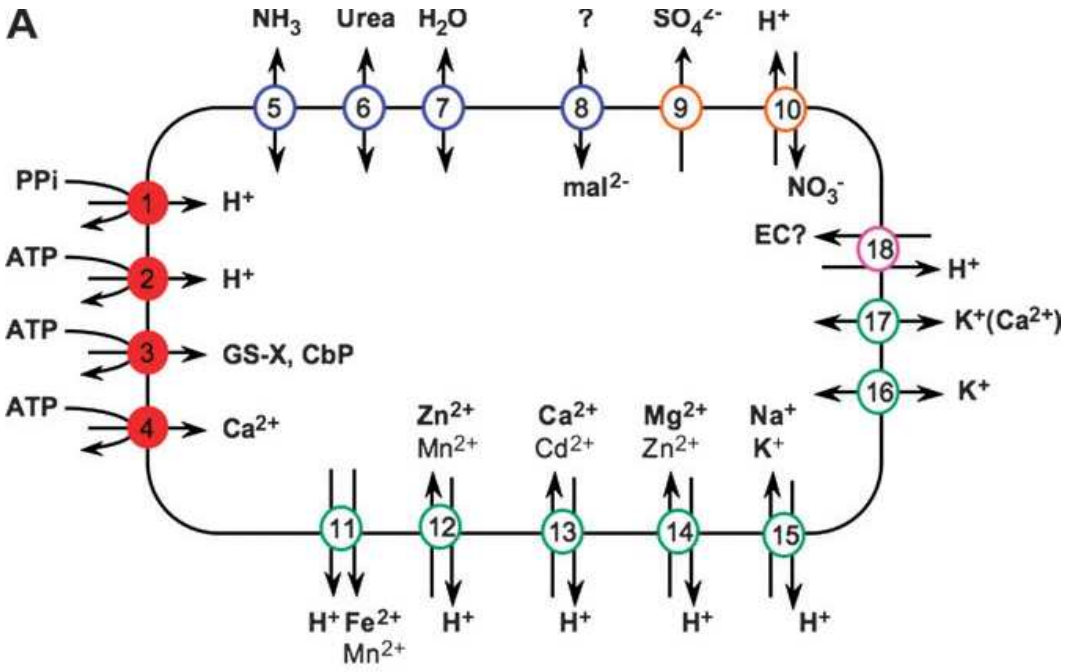

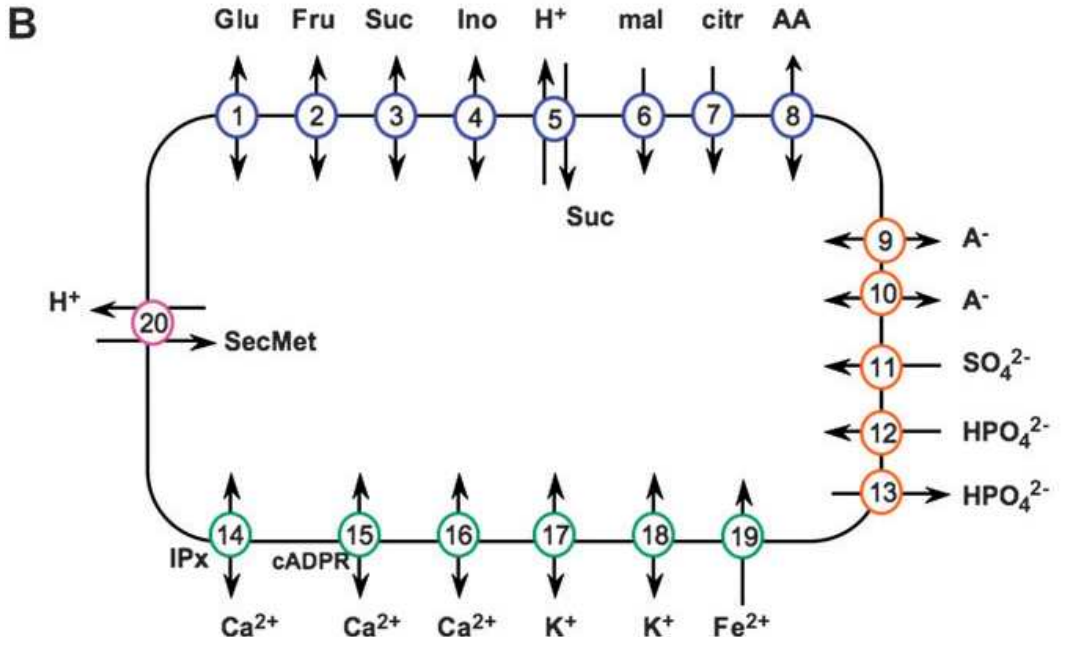

A – molekulárně char.
B - elektrofyziologie

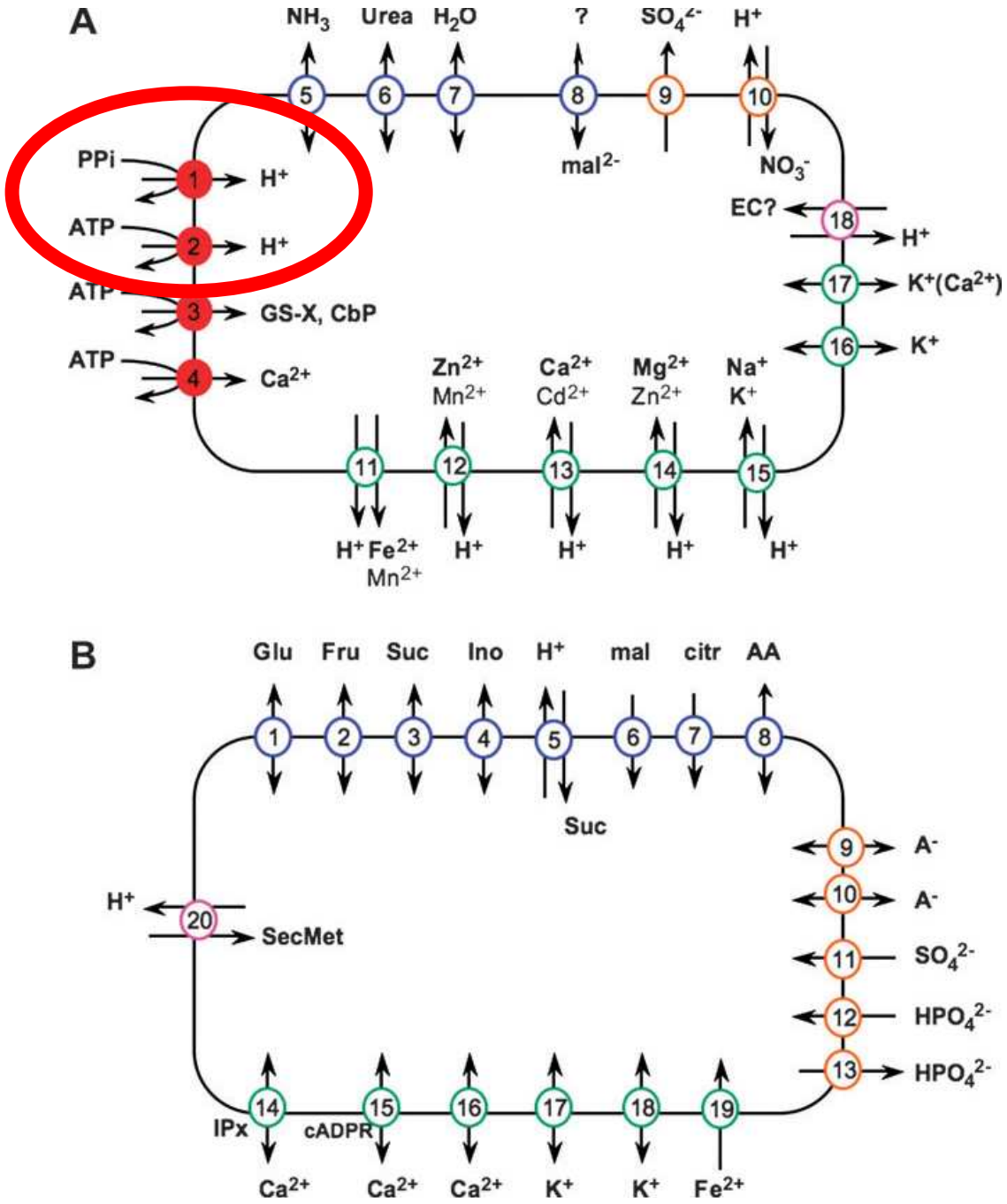

KANÁLY, PŘENAŠEČE A PUMPY TONOPLASTU

A – molekulárně char.
B - elektrofyziologie

Hlavní tvůrci Vm na tonoplastu.